Adv Polym Sci (2012) 246: 171–212
DOI: 10.1007/12_2011_141

Published online: 14 September 2011

Highly Aligned Polymer Nanofiber Structures: Fabrication and Applications in Tissue Engineering

Vince Beachley, Eleni Katsanevakis, Ning Zhang, and Xuejun Wen

Abstract Many types of tissue in the body, such as nerve, muscle, tendon, ligament, bone, and blood vessels, rely on a highly organized microstructure in order to impart their desired functionality. Cell and extracellular matrix (ECM) alignment in these tissues allows for increased mechanical strength and cell communication. In tissue engineering, aligned polymer nanofibers can be used to take on the role of natural ECM fibers in order to provide mechanical strength, sites for cell attachment, and modulation of cell behavior via morphological cues. A wide variety of physical and electrostatic techniques are available for assembly of aligned

V. Beachley and E. Katsanevakis
Clemson-MUSC Bioengineering Program, Department of Bioengineering, Clemson University, Charleston, SC 29425, USA

N. Zhang
Clemson-MUSC Bioengineering Program, Department of Bioengineering, Clemson University, Charleston, SC 29425, USA

Department of Microbiology and Immunology, Medical University of South Carolina, Charleston, SC 29425, USA

X. Wen (✉)
Clemson-MUSC Bioengineering Program, Department of Bioengineering, Clemson University, Charleston, SC 29425, USA

Department of Regenerative Medicine and Cell Biology, Medical University of South Carolina, Charleston, SC 29425, USA

Department of Orthopedic Surgery, Medical University of South Carolina, Charleston, SC 29425, USA

The Institute for Advanced Materials and Nano Biomedicine (iNANO), Tongji University, Shanghai 200072, People's Republic of China
e-mail: xjwen@clmson.edu

nanofiber structures, and many of these structures have been evaluated as tissue engineering scaffolds. It is widely understood that aligned microstructure induces an aligned morphology in most cell types, but aligned nanofibrous topography also influences other cell behaviors such as differentiation, gene expression, and ECM deposition. With a greater understanding of aligned nanofiber scaffold fabrication techniques, and cell interactions with these scaffolds, researchers may be able to overcome current challenges and develop better strategies for regenerating aligned tissues.

Keywords Characterization · Contact guidance · Fabrication · Nanofibers · Regeneration · Scaffold · Tissue engineering

Contents

1 Introduction

Natural tissues have a fibrous extracellular matrix (ECM) component made up of collagen, elastin, keratin, or other similar types of natural nanofibers. This nanofibrous ECM provides mechanical strength, storage locations for biomolecules, and structural support for cell attachment and organization. It also serves as a template for tissue formation during development, regeneration, and remodeling. For example, ECM deposition precedes cell migration in embryonic branching morphogenesis; nerve cells grow along aligned ECM tubes in peripheral nerve regeneration; and hydroxyapatite calcifies on collagen nanofibers to form bone during remodeling [1–3]. Polymeric nanofibers have received a great amount of attention in recent years due to their potential to fill some of the roles of ECM nanofibers in tissue engineering. Polymeric nanofibers have proven to be excellent substrates for cell attachment and growth, and the microstructure of polymeric nanofiber grafts can predictably modulate cell behaviors such as morphology, differentiation, ECM deposition, and migration [4]. In addition, the bioactivity of polymer nanofibers can easily be optimized due to a wide variety of available molecular compositions, methods of biomolecule incorporation, and surface modification techniques.

Many types of tissue, such as muscle, nerve, blood vessel, and connective tissue, require a well-aligned cellular and ECM organization for proper tissue function. Nerves are able to transmit signals throughout the body quickly through long well-aligned axons, and muscles, blood vessels, bone, tendons, and ligaments are able to apply and resist loads efficiently due to the aligned organization of cells and ECM fibers. Cells that are cultured in vitro on aligned nanofibrous scaffolds adopt an aligned elongated morphology that mimics the natural morphology of cell in aligned tissues in vivo. In addition to cell shape and organization, aligned nanofiber substrates have shown the ability to modulate cell behaviors such as differentiation, migration, and ECM assembly. It is of the highest importance that a tissue engineering scaffold used to mimic aligned tissues is able to impart uniaxial alignment in its resident cells in order to induce biomimetic organization and desired cellular responses. Challenges in tissue engineering applications of aligned nanofiber scaffolds include optimizing substrate topographical cues to promote desired cell responses and designing scaffolds with architecture conductive to the formation of tissue-like structures in vitro and in vivo.

Methods associated with many different fiber fabrication techniques are available for production of aligned nanofibers. However, the vast majority of research in this field is focused on aligned nanofiber fabrication using electrospinning. An overview of current aligned fiber fabrication technologies is presented, as well as a more detailed review of aligned fiber fabrication using the electrospinning technique. Cell interactions with aligned as compared to randomly oriented nanofibrous topographies are presented as well as specific tissue engineering applications of aligned nanofibrous scaffolds.

2 Methods of Fabricating Aligned Polymer Nanofibrous Structures

There are many techniques that utilize mechanical, electrical, or magnetic forces to align polymer nanofibers. Most aligning procedures are coupled with polymer nanofiber fabrication in a single step, while other are used to impart alignment to collections of nonaligned fibers post-fabrication. In the field of tissue engineering, the most common method of aligned nanofiber fabrication is electrospinning, but several other promising methods have also been explored for assembly of aligned nanofiber arrays. A brief overview of different methods of aligned nanofiber array fabrication is presented below.

2.1 Electrospinning

Electrospinning is an electrostatic method of fabricating polymer nanofibers that has generated widespread interest in the tissue engineering field due to its simplicity, immense versatility, and readiness for industrial scale-up. Electrospinning utilizes an electric field to eject a polymer solution or melt from a needle or small orifice as a thin liquid jet [5]. The electric field generates forces on the polymer solution that overcome surface tension forces in the needle, resulting in the ejection of a jet that is accelerated toward a grounded target. Violent whipping motions thin the jet as it travels toward the target and thus increase its surface area. A very high surface area to volume ratio promotes evaporation of the solvent, or cooling of a melt, resulting in the formation of polymer fibers at the target. When a flat target is used as the collecting area, a random fibrous mesh is formed, but many different variations of the electrospinning setup have been employed to allow fabrication of nanofibers with uniaxial alignment. There are two basic methods that are most commonly used to fabricate aligned nanofiber structures: (1) mechanical alignment using a high speed target, and (2) electrostatic alignment using a manipulated electric field. The preferred method of high speed target collection is the rotating mandrel technique and the preferred method of electric field manipulation is the parallel plate technique. The electrospinning technique will be discussed in further detail in Sect. 3.

2.2 Drawing

Polymer nanofibers can be directly drawn from a viscous polymer solution or melt when a droplet of polymer solution is mechanically stretched [6]. For example, the tip of a rod was dipped in a polymer melt and simply pulled out to form nanofibers with diameters as low as 60 nm and lengths up to 500 mm [7]. Resulting nanofibers can be manually oriented into aligned arrays or formed into arrays by automated

procedures [8]. A rotating collecting system was developed that can continuously draw a nanofiber from a nozzle and simultaneously arrange it into an aligned nanofiber array [9]. Polymer nanofibers with diameters ranging from 50 to 500 nm were formed into arrays with well-controlled diameter, alignment, and spacing using this system.

2.3 Extrusion

Continuous polymer fibers are formed when a polymer solution or melt is mechanically pushed with a ram through a die of desired cross-section. This method of fabrication is most commonly used in the textile industry, but conventional methods of fiber extrusion in the textile industry are not suitable for producing uniform polymer fibers in the nanometer diameter range. However, modified extrusion methods have been developed to successfully fabricate polymer fibers in the nanometer diameter range. Polymer nanofibers 100–200 nm in diameter and several micrometers in length were fabricated with a system utilizing air pressure to force 1–2 μm microsphere droplets though a steel mesh die [10]. In addition, continuous well-aligned polymer nanofibers with an average diameter as low as 424 nm were fabricated with a rotary system that utilized centrifugal force to push a polymer solution through a die [11]. The diameter of nanofibers produced by this method decreased as the rotational speed was increased.

2.4 Templating

Templating is a method used to fabricate arrays of uniaxially aligned nanofibers. Polymer solutions and melts are injected into alumina network templates by wetting, capillary forces, gravity, or extrusion [12]. Alumina network molds have been fabricated with pore diameters such as 25–400 nm and with pore depths ranging from 100 nm to several hundred micrometers [13]. Solid polymer nanofiber arrays are released from the molds after mold destruction or mechanical detachment [13, 14]. Nanofiber arrays produced by templating contain large areas of vertically aligned fibers of limited length that share a molded end base. Parameters such as fiber diameter, fiber height, and fiber spacing can be controlled by changing template dimensions and fabrication parameters such as melt time and temperature [15, 16]. The templating method can be used to fabricate surfaces with well-controlled properties, such as roughness, and wettability [15, 17]; however, nanofiber arrays fabricated by the templating method are not well suited for contact-guided cell alignment because of the limits in maximum fiber length. Templated fiber arrays are best suited for tissue engineering applications associated with surface chemistry, such as cell–substrate interaction studies and implant coatings [14, 16].

2.5 Micropatterning

Solution phase self-assembling nanofibers such as peptide amphiphiles (PA) have been observed to orient in aligned arrays when formed on micropattered surfaces. Aligned nanofiber assemblies have been observed on freshly cleaved mica surfaces [18], and the growth rate of PA fibers was quantified [19]. Large bundles of aligned PA nanofibers were assembled in an orientation parallel to patterned microchannels using a technique that incorporated sonication [20, 21]. Nanofibers fabricated by self-assembly are generally small compared to those fabricated by other techniques. Individual fiber diameters are several to tens of nanometers, and fiber lengths can reach several micrometers [4].

2.6 Fluid Flow

Fluid flow can be used to align polymer chains or precursors in solution, which become aligned nanofibers after subsequent solvent evaporation or polymerization. The mechanism of alignment is shear forces present in flowing fluids. Gravitational forces are easily utilized to generate fluid flow through dipping procedures that result in fiber alignment [22, 23]. Pressure driven fluid flow through pipettes and within microchannels has also been explored as a mechanism for forming aligned nanofibers [24–26]. Collagen fibers polymerized in 10–100 μm channels showed statistically significant alignment compared to controls when introduced to the channels under flow conditions, but not when introduced under static conditions [27]. Microchannel fluid flow was also combined with a drawing technique to produce aligned lipid nanotubes [28].

2.7 Magnetic Field-Assisted Alignment of Nanofiber Strands

High powered magnetic fields can be used to produce aligned nanofiber arrays from some materials. Magnetic alignment exploits anisotropy of the diamagnetic susceptibility of molecules. Several research teams have used strong magnetic fields to induce the alignment of cellulose [29, 30], collagen [31], and PA [32] nanofibers assembled under a strong magnetic field. The addition of magnetic beads allowed the fabrication of thin gels of aligned collagen using a small magnet [33]. This technique was used to induce collagen fiber alignment in plain and cell-containing gels several millimeters thick. It was hypothesized that the magnetic beads pulled fibers along the field lines formed by the magnet, resulting in a mechanism that might be similar to fluid flow alignment.

2.8 Surface-Induced Polymerization

Aligned nanofiber arrays can be directly produced during polymer synthesis with surface-induced polymerization reactions. Several types of polymers have been fabricated into nanofiber arrays on different substrates using surface-induced polymerization reactions [34–36]. Nanofibers were observed with lengths from a few hundred nanometers to several micrometerss and with diameters from 35 to 200 nm. Aligned nanofiber arrays formed by this method are vertically aligned and share a common base similar to those fabricated by the templating method.

2.9 Bacterial Cellulose

Cellulose nanofibers produced by bacterial cultures in vitro have found use in a variety of applications, including biomedical applications [37]. Potential advantages of bacterial cellulose nanofiber production include high yield and low cost. Cellulose nanofibers are synthesized by Acetobacter bacteria by a process that involves extracellular secretion of chains of polymerized glucose residues. Subsequent assembly of the chains and crystallization into ribbons results in networks of cellulose nanofibers with diameters less than 100 nm. Recently, methods of forming aligned nanofibrous networks with Acetobacter culture have been developed. Several groups found that bacteria cultured with various substrates were able to produced cellulose nanofibers with aligned orientations along the features of those substrates [38–40]. Large networks of aligned cellulose nanofibers were produced by Acetobacter when an electrical field was applied [41]. Aligned orientation was attributed to bacterial motion induced by the applied electric field.

2.10 Post-Fabrication Drawing of Nanofiber Arrays

A simple and intuitive way to impart alignment in randomly oriented nanofiber meshes is uniaxial stretching. When a randomly aligned nanofiber mesh is subject to a large uniaxial strain it can be transformed into an elongated aligned mesh. The mechanism of alignment is a mechanically induced reorientation of the randomly aligned nonwoven fibers in the direction of physical stretching. This technique, sometimes referred to as “post-drawing,” is used to impart or improve alignment in random or aligned nanofiber meshes. This technique is most commonly associated with electrospinning. In addition to reorienting fibers in the mesh, post-drawing can also elongate individual fibers, resulting in decreased fiber diameter [42]. In many cases, post-drawing procedures are conducted under elevated temperatures [42–44]. The post-drawing alignment mechanism has also been utilized in a modified electrospinning system to produce continuous uniaxial fiber bundle yarns [45].

3 Electrospinning of Aligned Nanofibrous Structures

The vast majority of publications related to the fabrication of aligned polymer nanofibrous structures and their application in tissue engineering involve the electrospinning fabrication technique. The two basic approaches used to obtain aligned nanofibers from an electrospinning jet are the rotating mandrel and parallel plate techniques. The rotating mandrel technique utilizes high velocities and mechanical tensile forces to impart alignment, while the parallel plate technique utilizes electrical forces to induce fiber alignment. The arrangement and composition of aligned nanofiber meshes collected by both techniques are influenced by the specific parameters of each electrospinning setup. In addition, a wide variety of modifications to these standard techniques have been explored in an attempt to discover more versatile aligned fiber fabrication methods. These modifications could facilitate the fabrication of better tissue engineering scaffolds by allowing better control over fiber length, alignment, placement, and three-dimensional (3D) organization.

3.1 Rotating Mandrel

The jet formed during electrospinning is ejected at a high rate of speed, reported as being up to several meters per second [46]. The deposition pattern of the high velocity jet can be controlled by using a target that is also moving at a high rate of speed. For this reason, the most common way of collecting aligned electrospun nanofibers, known as the rotating mandrel technique, utilizes a high speed grounded rotating mandrel as the collection target (Fig. 1a). Mandrel diameters are generally a few centimeters or larger and are rotated at speeds from zero to several thousand revolutions per minute (rpm). The tangential velocity is the most informative value to use when comparing different studies because mandrel diameters tend to vary significantly between studies. Relatively thick aligned fiber mats can be collected using this method, but the degree of alignment and the collection rate may decrease with mat thickness due to repulsive residual charges and the insulating effects of previously deposited nanofibers [47].

The speed of a rotating collector has several effects on the microstructure of collected fibers and their spatial arrangement. It is hypothesized that when the tangential velocity at the edge of a rotating mandrel matches the speed of the electrospinning jet, the degree of alignment will be maximized [48]. Fiber orientation resulting from different mandrel velocities can be classified in three stages: (1) mandrel velocity is too low to initiate fiber alignment, (2) mandrel velocity initiates increasing fiber alignment with increasing speed to a maximum, and (3) fiber alignment decreases due to fiber fracture caused by extreme velocities [49]. The threshold speed for fiber alignment is different from system to system. Several groups using various synthetic polymers saw the onset of fiber alignment at around 3 m/s [50–53], whereas others have required speeds approaching 10 m/s [54] for the

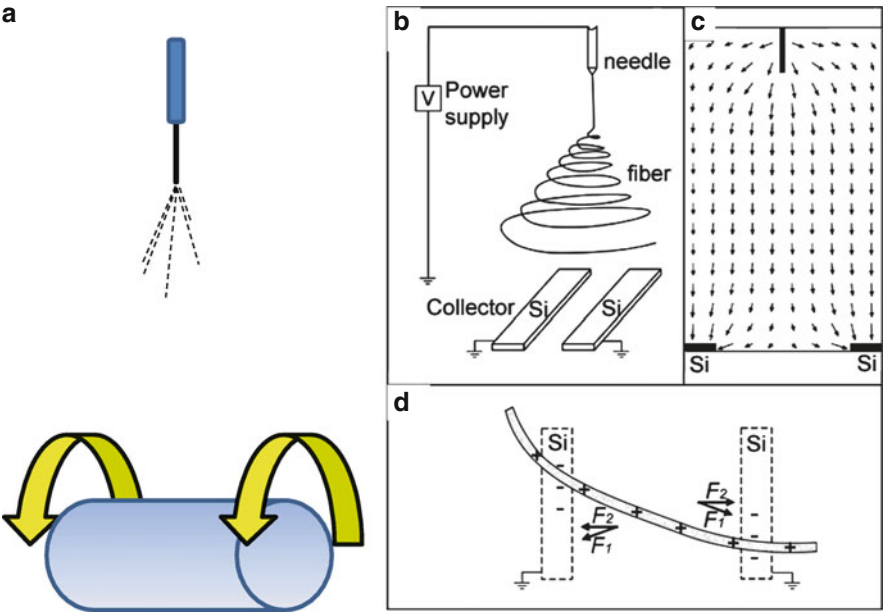

Fig. 1 Setup for electrospinning aligned nanofibers using the (**a**) rotating mandrel, and the (**b**) parallel plate techniques. (**c**) Calculated electric field strength vectors and (**d**) electrostatic force (F) analysis associated with the parallel plate techniques [62]

onset of alignment. The degree of alignment generally increases with increasing tangential velocity after the onset of fiber alignment [50–56]. As mandrel speeds continue to increase, fibers may begin to break due to tensile forces exerted by the mandrel on the fibers [54]. Fiber breakage can result in decreasing fiber alignment and quality [48]. The mandrel speed associated with fiber breakage is dependent on the material properties of the electrospun polymer and it has been shown that nanofibers electrospun from brittle materials are more likely to break at lower mandrel speeds [57].

The tensile force exerted on the electrospinning jet by a rotating mandrel can result in a reduction of fiber diameter for deformable materials. Fiber diameter generally decreases with increasing mandrel speed [50, 54–56, 58, 59], although slight increases in diameter have been observed under certain conditions [49, 60]. Reported fiber diameter reductions of around 15–40% versus static collection have been observed when mandrels were rotated at 5–15 m/s [50, 54–56, 58, 59]. Though the exact tangential velocity must be determined in order to allow maximum alignment, the tensile force exerted by the rotating mandrel also affects the fiber diameter and can even influence fiber molecular orientation [49, 61]. This must be taken into account when deciding on an optimal mandrel speed.

Despite a general agreement for some trends related to mandrel effects on fiber microstructure, it is difficult to precisely predict how a rotating mandrel will affect nanofiber structure for a specific system due to the amount of variables involved.

Fiber jet speed and material elasticity are two of the most important parameters involved in the jet–mandrel interaction and each of these properties are influenced by multiple electrospinning parameters, such as solution conductivity, viscosity, voltage, and feed rate. In addition, material properties cannot be accurately predicted without knowing the exact degree of solvent evaporation at the point when fibers are taken up by the collector.

3.2 Parallel Plate

Another method of collecting aligned nanofibers is by manipulation of the electric field in the collecting area. The highly charged electrospinning jet is sensitive to the surrounding electric field and will align in certain electrical field configurations. The most commonly used method of aligning nanofibers with an electric field is the parallel plate technique. When two grounded parallel plates are set up as the collecting target they create an electric field that causes deposition of nanofibers aligned perpendicular to the plates across the air gap between them. Analysis of the electric field present in a parallel plate electrospinning setup and the resulting forces exerted on the electrospun nanofibers was first conducted by Li et al. [62]. Diagrams of this analysis are displayed in Fig. 1b, c. The electrical properties of the polymer solution become increasingly important when electrospinning nanofibers across parallel plates because electrostatic forces are responsible for aligning the fibers. Many polymer solutions that are easily electrospun into nanofibers on a flat target do not align well on parallel plates because the solution properties do not facilitate good alignment with the electric field.

It can be hypothesized that the electrical properties of a polymer solution must be within a critical range to facilitate effective deposition across parallel plates. If a solution's conductivity is too low, the electrostatic forces may not be sufficient to pull fibers across the gap; but if it is too high, then random whipping instabilities may dominate the motion of the jet. For example, it was hypothesized that fiber collection across parallel plates was ineffective for an electrospun polyelectrolyte solution [poly(phenylene vinylene), PPV] because its high conductivity contributed to a highly unstable jet that could not be effectively stabilized by the aligning forces at the collection site [63]. Addition of a neutral polymer (polyvinyl pyrrolidone, PVP) to this solution allowed the formation of well-aligned nanofibers (Fig. 2a–c). In another study, it was hypothesized that parallel plate fiber collection became ineffective after the addition of NaCl to the polymer solution due to jet instabilities caused by increased solution conductivity [64]. Nanofibers electrospun from a melt were aligned only at gap distances less than 1 cm and collected as randomly oriented meshes at greater gap widths [65]. In this case, the forces exerted by the electric field on the solution may have been too small to result in alignment due to low conductivity.

Electrostatic forces exerted on an electrospun jet can be controlled independently of solution properties by changing the applied voltage. An increase in the

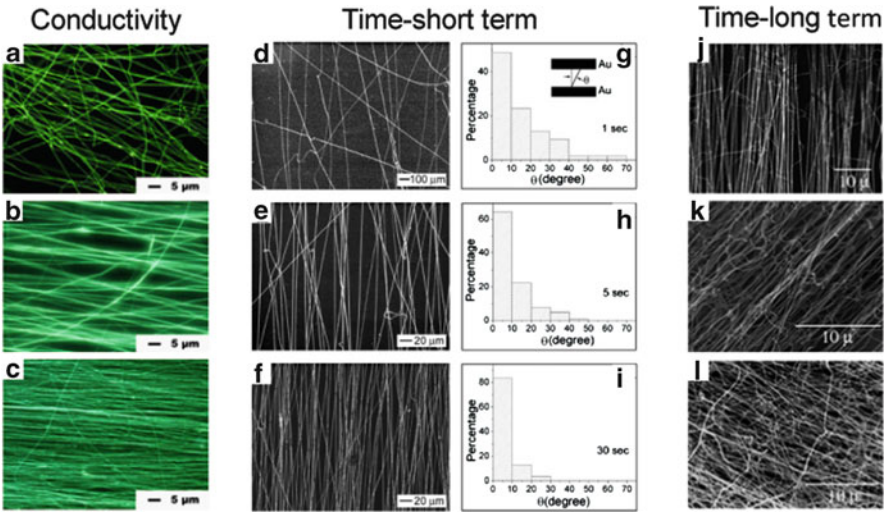

Fig. 2 Fiber alignment increased with decreasing solution conduction for (**a**) pure PPV, (**b**) PPV/PVP 50:50, and (**c**) PPV/PVP 20:80 [63]. Fiber alignment increased with time from (**d**, **g**) 1 s, to (**e**, **h**) 5 s, to (**f**, **i**) 30 s [67]. Fiber alignment decreased with increasing time from (**j**) 5 min, to (**k**) 15 min, to (**l**) 2.5 h [71]

voltage of an electrospinning setup results in an increase in the electric field strength and thus an increase in the forces acting on the fibers. However, increased voltage also increases the jet instability, which may decrease fiber alignment. Therefore, a critical voltage that balances the magnitude of the aligning forces and the resultant jet instabilities must be obtained for optimal fiber deposition and alignment across parallel plates [66].

Another limitation that is specific to the parallel plate electrospinning technique is the collection of extremely thin nanofibers, which have been observed to break because they were unable to sustain the forces of their own weight and of the repulsive charges from other fibers [62]. An electrically resistive substrate inserted into the gap between the plates can provide support to fibers suspended between the plates without influencing fiber quality [62], and may also help to shield any conductive materials below the air gap, which may attract unwanted non-aligned nanofibers. Substrates with bulk resistivity greater than 10^{22} Ω cm, such as quartz and polystyrene, are suitable for placement between parallel electrodes, while materials with bulk resistivity of less than 10^{12} Ω cm, such as glass, may result in random fiber orientations [67, 68].

3.2.1 Charge Retention

Nanofibers collected in full contact with a conductive electrode immediately discharge. However, fibers suspended in air across parallel plates retain charge

throughout the portion of the fiber that does not have contact with the conductive plates [62]. The accumulation of both charge and material in between the gap has a significant effect on the electric field, thus the fiber deposition patterns are constantly changing as fiber density increases. Charge retention can have effects on subsequent fiber alignment and collection rate due the repulsive forces exerted on the electrospinning jet. Residual charge can initially improve alignment in low density arrays because parallel alignment is the lowest energy state of an array of charged fibers [62, 67, 69]. Improved alignment at various time points up to 30 s are shown in Fig. 2d–i [67]. Numerical models are in agreement with the positive effects that residual charge has on alignment at low fiber densities [70]. However, over longer periods of fiber collection, as fiber density increases, the alignment of subsequent fibers can become poor due to build-up of charge and materials (Fig. 2j–l) [71]. As fiber density continues to increase, the charge repulsion and material build-up can resist further fiber deposition between the parallel plates almost entirely. Therefore, thick layers of aligned fibers are difficult to fabricate by this method [72].

3.2.2 Gap Size and Plate Geometry

The electric field and thus the collection dynamics of parallel plate electrospinning setups are affected by the geometry of the parallel plate configuration. The gap size has an especially significant role in fiber alignment and array density. The draw of the aligning electrostatic forces created by parallel plates decreases with increasing gap distance, making it is more difficult to collect aligned nanofibers across a larger distance [73]. Although nanofibers as long as 50 cm have been collected across parallel plates, fiber density and rate of deposition generally decrease with increasing gap distance until no fiber collection is possible [74, 75]. Collection of densely aligned nanofiber arrays becomes infeasible as gap size increases due to decreasing electrostatic forces and charge repulsion. Because of the gap size limitations, fiber length in high-density aligned nanofiber arrays is usually limited to a few centimeters. Nanofibers electrospun across various gap distances from 3 to 6 cm demonstrated a highly reduced fiber array density with increasing gap distance [66, 69].

Gap distance also has an effect on fiber alignment. As the gap size increases, fiber alignment may initially increase and then decrease with a critical value of maximum alignment. The critical values of maximum alignment for two different electrospinning systems were 1 and 3 mm [66, 73]. Reported results on the effect of gap distance on alignment can vary significantly from study to study, which is not surprising due to the many components involved in fiber alignment across parallel plates. For example, alignment was observed to increase with an increase in gap distance from 2 to 6 cm with one electrospinning system [69], and decrease with an increase in gap distance from 0.5 to 2.5 cm with another system [64].

3.2.3 Effects of Electrostatic Forces on Fiber Morphology

The columbic forces that align electrospun nanofibers across two parallel plates exert a mechanical force much like the mechanical tensile forces exerted by a rotating mandrel. Like the rotating mandrel, parallel plate collection sometimes results in nanofibers with reduced diameters compared to those formed using flat plate collection. Whereas the magnitude of the force in a rotating mandrel is set by the speed of the collector, the magnitude of the force in a parallel plate system is set by the strength of the electric field and the electrical properties of the jet. It can be anticipated that electrospinning setups that incorporate large electrostatic forces or more deformable materials may result in a more pronounced decrease in fiber diameter. The diameter of nanofibers collected across a parallel plate decreased with increasing concentrations of carbon nanotubes [76]. This result is anticipated because the forces pulling the fibers across the parallel plates should increase with increasing nanotube concentration due to the increased conductivity of the solution. Fiber diameter decrease for parallel plate collection was also especially pronounced for melt electrospinning, which could be due to the deformability of hot fibers that had not fully cooled before alignment [65].

3.3 Challenges in Electrospinning Aligned Nanofiber Structures

Both the rotating mandrel and parallel plate technique have advantages and disadvantages. The rotating mandrel can be used to collect large-area thick mats of aligned fibers, but highly aligned assemblies may be difficult to fabricate and the fiber arrays may be tightly wound or broken due to high rotation speeds [72]. The parallel plate technique allows easy transfer of fiber arrays to other substrates, but this technique is sensitive to solution properties and there are limitations in array fiber density and thickness and in fiber length [72]. These limitations constrain the specific types of aligned structures that can be fabricated by electrospinning and reduce the applicability of this technique. Many interesting innovations have been developed to address these limitations and allow greater control over fiber array deposition area, fiber alignment, continuous fiber length, fiber mat density, and yield.

3.3.1 Focusing and Steering the Electrospinning Jet

Under normal electrospinning conditions, the deposition area of an electrospinning jet can be undesirably large and difficult to predict. This can lead to difficulties in precise and repeatable fabrication of uniform nanofiber arrays, and materials may be wasted. It is desirable to explore methods to control the deposition of an electrospinning jet in terms of both focused fiber deposition area and controlled placement of the fiber deposition area. The range of fiber deposition is usually decreased as the needle-to-collector distance is decreased; however, this alone may

not provide the desired level of fiber deposition focus and may result in unwanted side effects [77]. Several technologies such as repulsive electric fields, sharp-edged collectors, and attractive oppositely charged electrodes have been applied to focus and control the deposition location of an electrospinning jet.

The area of aligned nanofiber deposition can be focused by confinement and general stabilization of the whipping motions of the electrospinning jet early in its trajectory. Objects with the same charge as an electrospinning jet exert a repulsive force on the jet, and when placed in a proper configuration can produce an electrostatic force that acts as a barrier to confine the jet. Positively charged rings, cylinders, and plates have been placed around an electrospinning jet to electrostatically confine it and reduce the final fiber deposition area at the collection target [78–80]. In one instance, the diameter of randomly deposited nanofiber mesh was reduced from 7 to 1 cm with the addition of positively charged ring electrodes placed around the electrospinning jet path [80].

The deposition area can also be focused using a thin sharp-edged collector. A thin sharp edge confines the actual area for fiber deposition, and focuses the electric field (Fig. 3), promoting a narrow deposition of fibers [81]. Several groups have used thin rotating disks in place of a standard rotating mandrel to collect thin highly aligned nanofiber bundles. A system similar to a sharp-edged disk employed a thin wire wrapped around spokes connected to a rotating mandrel [82]. In a variation of that technique, a wire can be wrapped around an insulating cylinder to allow collection of multiple focused aligned nanofiber arrays simultaneously [83]. Thin sharp edges have also been used in the configuration of a parallel plate

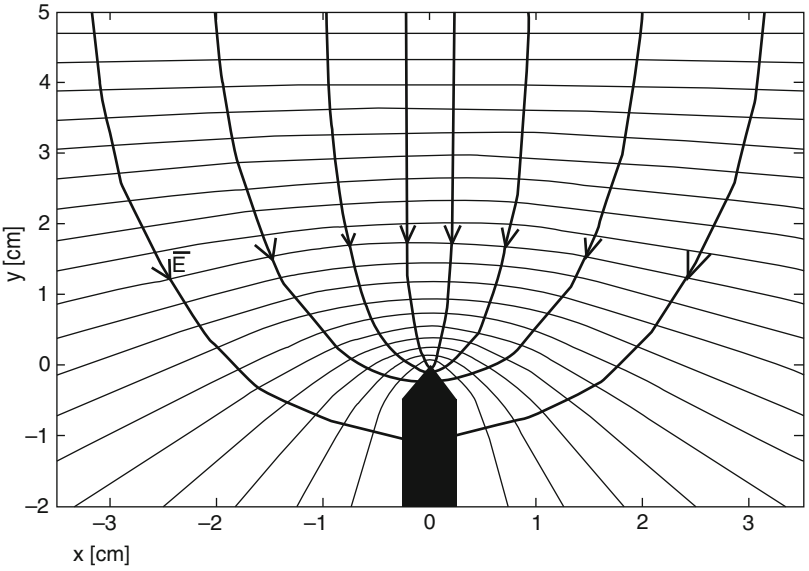

Fig. 3 Electrostatic field simulation for a sharp-edged collector. Equipotential lines of the electric potential and electrostatic field lines are plotted [81]

collector. Two steel blades placed upright in a direction perpendicular to a standard parallel plate setup were used to collect thin aligned nanofiber arrays at gap distances up to several centimeters [75], and sharpened parallel plates were able to attract a greater quantity of fibers than standard parallel plates [84].

Another method of focusing and controlling the deposition of an electrospun nanofiber array is to use an oppositely charged auxiliary electrode to attract the jet. Electrospinning systems using this technology are generally arranged so that a collecting mandrel is placed between the nozzle tip and the oppositely charged electrode (Figs. 4 and 5). Narrow aligned nanofiber arrays were fabricated on the surface of a rotating mandrel when an oppositely charged pin electrode was placed immediately behind or inside of it [85, 86]. It was found that the width of the aligned fiber deposition area on the collector narrowed with decreasing collector to spinneret distance and increasing field strength [77]. Parallel arrays of oppositely charged strip

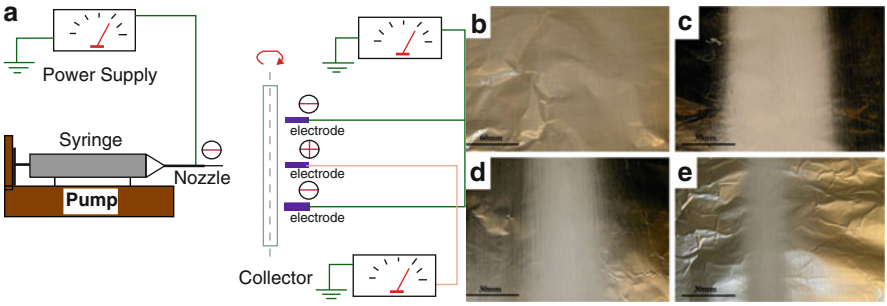

Fig. 4 (**a**) Electrospinning setup with counter electrodes used to focus the area of fiber deposition. (**b**–**e**) Images of resultant nanofiber mats electrospun with (**b**) no auxiliary electrodes, (**c**) one auxiliary counter electrode, and (**d**, **e**) both counter and like electrodes with different separation distances between them [48]

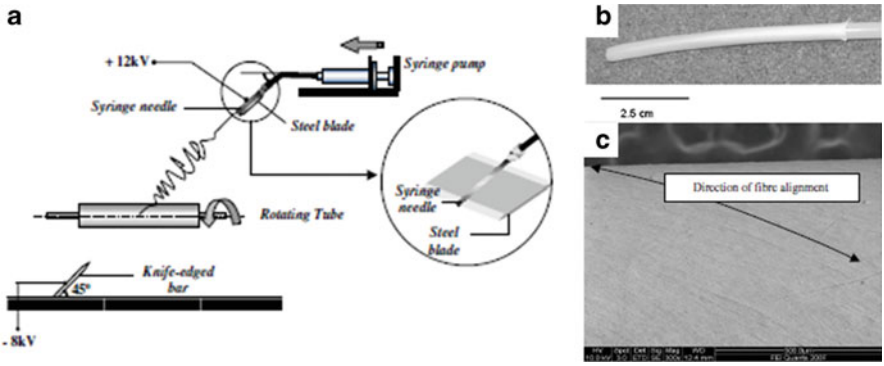

Fig. 5 (**a**) Electrospinning setup using an auxiliary counter electrode to direction the path of an electrospinning jet. (**b**, **c**) A tubular structure with diagonally oriented aligned nanofibers was fabricated when a mandrel was placed in the path of the jet at an angle [87]

and sharp-edged bar electrodes have also been placed below rotating mandrel collectors to confine aligned nanofiber array deposition [87, 88]. Electrode arrays containing both like and opposite charges can be arranged to focus the deposition area even more effectively. The width of a nanofiber array collected on a rotating mandrel was reduced by up to 60% when two like-charged electrodes (same charge as the jet) were placed on each side of an oppositely charged counter electrode (Fig. 4) [48]. Oppositely charged electrodes are also capable of patterning the location and arrangement of aligned nanofiber deposition on a rotating mandrel. The attractive force between an electrospinning jet and an oppositely charged electrode is strong enough to redirect the direction of the jet to the position of the electrode, even if it is not located directly below the nozzle [85]. When the counter electrode is positioned off-center relative to the nozzle, the electrospinning jet can be forced to take a trajectory at an angle to the rotating mandrel and allow collection of aligned fiber arrays with various angular orientations (Fig. 5) [87]. Therefore, precisely oriented aligned nanofibers can be honed to a specific axial location on a rotating mandrel. Lateral translation of either the oppositely charged electrode or the mandrel itself allows dynamic control of fiber deposition over the entire mandrel [86].

3.3.2 Fiber Alignment

Generally, the methods of fiber array confinement described above also result in improved array alignment due to geometrical constraints and the focused electric field. When the nanofiber jet is focused there is less probability for misalignment, and the increased electrostatic forces generated may improve fiber alignment control. Specific examples of improved fiber alignment exist for each of the three general methods described above. A confining electric field generated by two like-charged plates applied around an electrospinning jet was observed to improve deposited fiber alignment across parallel plates [78]. When a thin blade is used as the collecting surface, a greater percentage of aligned fibers may be collected because unaligned fibers might miss the target or only a small portion of the fiber will cross the thin blade. In addition, the increased electrostatic force generated by thin blade collectors can improve fiber alignment independently of geometrical constraints [87]. Improved fiber alignment has also been observed when oppositely charged counter electrodes were added to a conventional rotating mandrel setup. This resulted in aligned nanofiber collection at lower speeds [48].

Other methods have been developed to improve fiber alignment in nanofiber arrays of larger area. One innovative way to increase fiber alignment using the parallel plate technique is to apply an alternating potential to the two collection plates. Initially, the nanofiber jet is more attracted to one plate than to the other. When the field is switched the jet moves to the other plate, and oscillation guides fiber deposition back and forth across the plates (Fig. 6) [89–91]. In one configuration, an AC potential is applied to one plate, while the other remains grounded [89, 90]. A different configuration utilized high voltage reed relays or switches to alternate charge and ground between two parallel plates [91, 92]. This configuration has been

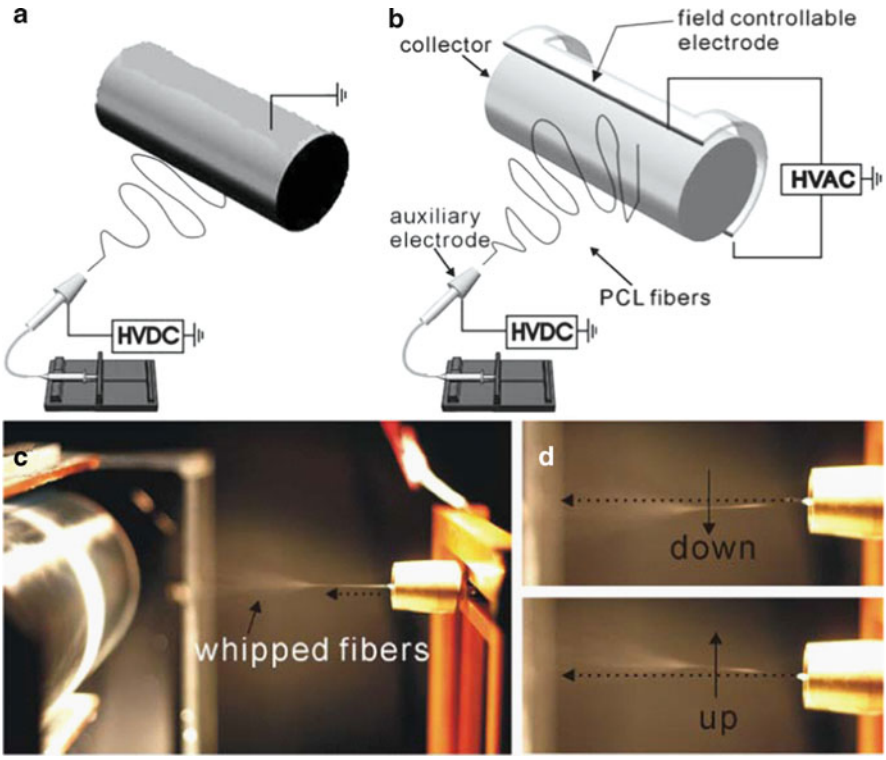

Fig. 6 Electrospinning with (**a**) normal rotating mandrel compared to (**b**) modified system with AC field controllable counter electrode. (**c**, **d**) The effect of the AC electrode on the jet is shown, where (**c**) corresponds to a normal setup and (**d**) is with the AC electrode [89]

used with both repulsive (same charge as jet) voltage/ground and attractive (opposite charge as jet) voltage/ground alternations between plates [91, 92]. Orientation may be affected by the frequency of the applied field, with an optimum frequency for maximum alignment [79, 89].

Interestingly, when an AC potential is applied to the electrospinning nozzle instead of a DC potential, fiber alignment on a rotating mandrel can also be improved. It is hypothesized that this could be due to decreased net charge and thus decreased jet instability [93]. Further investigation into this technique showed that addition of a DC potential biased to an AC potential improved the quality and alignment of nanofibers collected on a rotating mandrel as compared to AC or DC potentials alone [94].

3.3.3 Fiber Length

Verifiable single continuous nanofibers can be fabricated by the parallel plate method. Increasing the maximum length of fibers that can be collected across

parallel plates may increase the applications of this method. Long nanofibers up to 50 cm were collected using a parallel plate setup with very large plates (30.5 × 7.5 × 0.7 cm), and maximum fiber length was observed to increase with increasing plate size [74]. It was hypothesized that even longer fibers could be collected with larger plates. External forces can also be utilized to suspend long nanofibers across a gap. Long suspended nanofibers (25 cm) were formed when a nanofiber jet was shot sideways and adhered to a raised target at one end, while the other end was pulled down by gravity and adhered to a support [95]. Another system utilized gas flow to pull one end of an adhered nanofiber toward an electrode to suspend it across a long gap (>20 cm) [96].

3.3.4 Fiber Density and Thickness (Parallel Plate)

A major limitation of the parallel plate technique is limited fiber density and mat thickness, as explained in Sect. 3.2.1. This problem can be overcome by utilizing other forces that are able to overcome the electrostatic repulsive force between nanofibers. Thick aligned nanofiber mats were fabricated across parallel plates when a magnetic field was used to attract fibers to a mesh across parallel plates [97]. Another technique utilized mechanical forces to assemble low density aligned fiber arrays into thicker constructs [98]. This technique used automated tracks to provide continuous mechanical assembly of fiber arrays, and allows theoretically infinite mat thicknesses.

3.3.5 Yield

In order to be practical for industrial scale-up, aligned fiber fabrication should have a high yield. The simplest method of maximizing yield for both the parallel plate and rotating mandrel techniques is the use of multiple spinnerets to deposit aligned nanofibers over long sections of rotating mandrel or parallel plate simultaneously [99–101]. It is important to consider interference between the jets when multiple spinnerets are used because like-charged jets repel one another and oppositely charged jets attract one another [102]. Another method of increasing yield is to move the collecting surface. Several groups have translated rotating mandrels normal to the electrospinning jet to increase the area of coverage [86, 101, 103]. Multiple parallel plate-type aligned nanofiber arrays can be collected simultaneously when a rotating wire mandrel collector is used [71, 104]. In this case, the wire spokes act as individual parallel plate collectors and, as the wire mandrel rotates, different parallel wire gap locations are present directly beneath the electrospinning nozzle [105]. Similar to the wire frame technique, a rotating mandrel with fins has been used to fabricate many suspended aligned nanofiber arrays simultaneously [42]. Parallel plates have also been put into motion to increase nanofiber yield. When two parallel plates are replaced by two parallel conductive tracks moving normal to an electrospinning nozzle, continuous aligned nanofiber array production across the tracks is possible [98].

4 Cell Interactions with Aligned Nanofibrous Structures

Cell morphology is highly sensitive to nanofibrous topography. Cells adopt different shapes on nanofibrous surfaces than on flat surfaces, and fiber diameter and orientation further modulate cell configuration [4]. Aligned cell morphologies commonly observed on aligned nanofibrous substrates are especially important in designing tissue engineering environments that mimic aligned tissues such as nerve, muscle, ligament, and tendon. In addition to the practical advantages of alignment in such tissues, variations in cell morphology generally correspond to changes in cytoskeletal arrangement that can further modulate other cell behaviors such as elongation, proliferation, migration, ECM production, and differentiation.

4.1 Cell Morphology and Alignment

Cell orientation on nanofibrous substrates is generally described as rounded or polygonal, which corresponds to a lack of organized actin fibers, or as elongated or spindle-shaped, which corresponds to well-organized actin fibers in the direction of elongation [52, 106]. These morphologies are in contrast to the flat well-spread shape seen on flat surfaces [106]. Elongated cell morphology can be quantified by its aspect ratio, which is the ratio of the length of the cell's long axis to its short axis. The dependence of cell morphology on substrate fiber orientation has been quantified as a systematic increase in aspect ratio as fiber orientation progresses from random to aligned [50]. Quantification of cell morphology varies greatly for specific cell types, substrates, and culture times, but in one representative example, cell aspect ratio on highly aligned nanofibers was quantified as twice that seen on randomly oriented nanofibers and three times that seen on a glass control 24 h after seeding [52].

The angular direction of cell elongation corresponds to the direction of the underlying fibrous substrate and, thus, cell populations cultured on well-aligned nanofibrous substrates are well aligned in relation to one another. Most cell types, including neural, muscle, fibroblast, endothelial, and mesenchymal stem cells (MSCs), adopt an aligned morphology when cultured on aligned nanofibrous substrates [56, 103, 107–111]. According to several studies, the quantitative degree of cellular alignment generally corresponds to the degree of underlying fiber alignment [50, 59, 112–114]. Among these studies, quantitative cell alignment values were reported to be slightly higher, lower, or near identical to that of the underlying fiber substrates. A representative distribution of cell and fiber orientation is displayed in Fig. 7 [114]. Cells can organize into an aligned orientation soon after they attach to an aligned nanofibrous substrate. MSCs and fibroblasts were organized in the direction of the underlying fibrous substrate after 24 h in culture, and a more detailed observation of C2C12 cells revealed F-actin organization into parallel stress fibers after just 30 min, with substantial cell elongation after 2 h (Fig. 8) [52, 56].

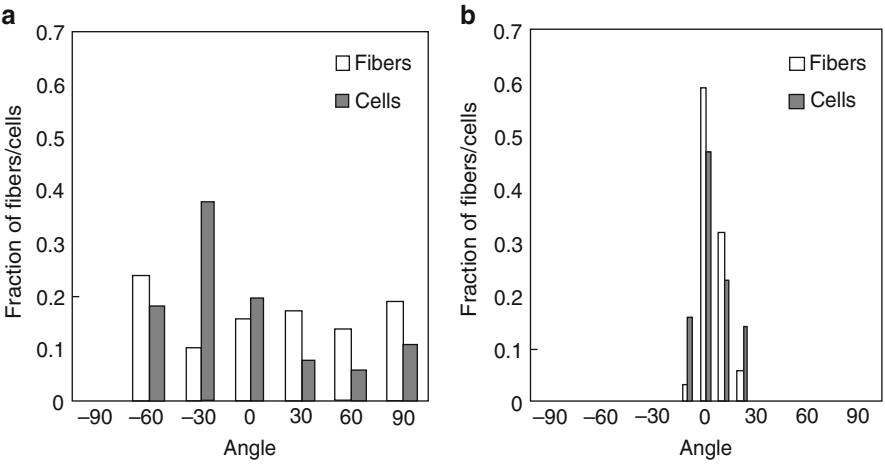

Fig. 7 Angular distribution of nanofiber substrates and the cells cultured on them are shown in normalized histograms. (**a**) Substrate was collected on a solid plate, and (**b**) substrate was collected on a rotating mandrel [114]

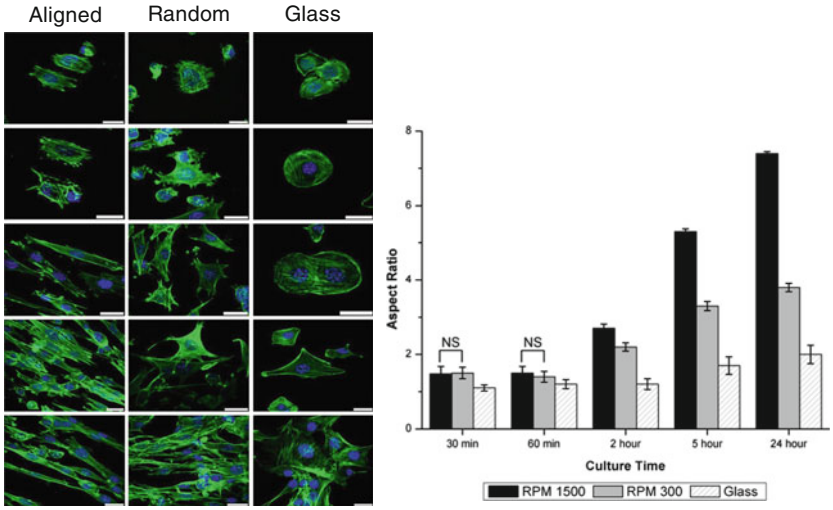

Fig. 8 *Left*: C2C12 cells were seeded on aligned and randomly oriented fibers and on a glass control. Confocal images taken at 30 min, 60 min, 2 h, 5 h, and 24 h after seeding are shown, with increasing time from *top* to *bottom*. Actin is stained *green* and nuclei are stained *blue*. *Scale bar*: 25 μm. *Right*: Quantification of cell aspect ratio is shown for all time points. All data sets are significantly different from each other except those indicated by *NS* [52]

Cell alignment parallel to aligned nanofibrous substrates is consistently observed in many studies, even though different cell types and different types of nanofibrous materials have been employed. However, there are some interesting exceptions.

Table 1 Neural cell elongation on aligned nanofiber substrates

Reference	Cell type	Culture time (days)	Max. length	% Increase[a]
[113]	Rat DRG E15	3	760 μm	20
[118]	Rat DRG P4-P5	6	3.5 mm	300
[119]	Chick DRG E9	5	11 mm	500
[117]	Mouse NSC C17.2	2	95 μm	100
[107]	Mouse NSC C17.2	2	100 μm	25
[120]	Mouse NSC CE3/RW4	14	1.7 μm	40
[121]	Human NSC H9	7	450 μm	300

[a]Increase in elongation of neural cells on aligned nanofibrous substrate as compared to randomly oriented nanofiber substrate

Neurites growing on a nanofibrous scaffold inserted in the brain were observed to preferentially align in the direction perpendicular, not parallel, to the aligned nanofibers [115]. Interestingly, a small but surprisingly significant amount of neurites grown in vitro also oriented perpendicular to the aligned nanofiber direction: 94% parallel, 4% perpendicular, 2% intermediate [107].

4.2 Cell Elongation

Cell elongation is closely related to cell shape, but also accounts for accelerated cell growth or maturation. Elongation is an especially important property in skeletal muscle and neural tissue engineering, where native cell types may reach lengths of several centimeters or more than a meter, respectively. Aligned nanofibrous substrates are consistently reported to promote accelerated elongation in neural cells as compared to randomly aligned substrates, (see Table 1). Myotube length on aligned nanofibers was also observed to be twice that seen on randomly aligned scaffolds, while myotube thickness remained similar [110]. Furthermore, the fiber diameter of aligned nanofiber scaffolds has a significant effect on the rate of elongation. 3T3 fibroblast elongation on single fibers increased systematically as fiber size decreased from 10 μm to 500 nm, with a 50% increase in length when fiber diameter was reduced from 4 μm to 500 nm [116]. Neural stem cells (NSCs) also increased in length with decreasing fiber size. Two similar studies demonstrated a 25% increase in neurite length when fiber diameter was reduced from 1.5 μm to 300 nm [107], and a 70% increase in neurite length when fiber diameter was reduced from 917 to 500 nm [117]. There is evidence that a critical value of optimum fiber diameter may exist because maximum neurite elongation on aligned nanofibers with diameters of 307–917 nm was determined to be around 500 nm [117].

4.3 Cell Proliferation

Cell proliferation is a vital process in tissue regeneration. It is generally desirable to maximize cell proliferation in tissue engineering scaffolds, but in some cases, such

as astrocyte proliferation at a neural tissue–implant interface, minimization of cell proliferation may be desired. In designing tissue engineering scaffolds it is important to be able to understand the effects of scaffold microstructure on cell proliferation.

It is well documented that nanofibrous microstructure can have an effect on cell proliferation; however the effect is quite varied across different studies using different types of scaffolds and cell types. When comparing nanofiber substrates versus flat controls, cell proliferation was higher on nanofibers in several studies [122, 123] and higher on flat control in several others [124, 125]. The specific fiber diameter of nanofiber substrates also has been shown to have varied effects on cell proliferation [126–129]. Similarly, the effect of nanofiber orientation on cell proliferation varied greatly between individual studies. Cell numbers on aligned nanofiber scaffolds have been observed at significantly higher values of up to twice those seen on randomly aligned control scaffolds after 3–70 days of culture [54, 123, 130, 131]. In contrast, no significant difference in cell proliferation for different degrees of fiber orientation was observed in several other studies over 3–21 days [50, 59, 112, 114, 132–134].

Unfortunately it becomes very difficult to quantitatively analyze the effects of nanofiber microstructure and orientation on proliferation because of factors inherent to these types of scaffolds that can interfere with results. Cell proliferation may be induced by substrate signals transduced through the cytoskeleton, or cell numbers may simply be increased because of spatial considerations. Cell morphologies induced by substrates with certain fiber orientations may allow higher monolayer cell packing density, or certain fiber orientations may allow greater cell penetration and expansion into the volume of the scaffolds.

4.4 ECM Production

Although aligned polymer nanofibers have some similarities to natural ECM, it is vital to tissue regeneration that resident cells produce their own natural matrix to compliment or replace the engineered scaffold. Substrate microstructure has pronounced effects on both the amount of ECM produced by resident cells and the architecture of that matrix. Increased ECM production has been observed in cells cultured on nanofibrous substrates compared to those on flat substrates and large (15 μm) microfibers [106, 135]. The specific fiber diameter of nanofibrous substrates may also affect the ECM production of attached cells [129].

The orientation of nanofibrous substrates modulates ECM production by resident cells in both quantity and quality. Increased calcium and collagen production were observed when cells were cultured on aligned nanofibers as opposed to randomly oriented scaffolds [114, 132, 133]. However, in other cases, the magnitude of ECM production was unaffected by nanofiber substrate orientation [59, 130, 132]. In addition to increasing the magnitude of ECM production, nanofibrous substrates may also promote ordered arrangement of synthesized ECM similar to that seen in

natural tissues. Quantitative analysis of the collagen I matrix produced by fibroblasts cultured on nanofiber scaffolds revealed a linear orientation for aligned scaffolds that was not present for randomly aligned substrates [112]. Optimized collagen arrangement may result in improved function in regenerated tissue. A 10-week fibroblast culture on nanofiber scaffolds resulted in an increase in scaffold mechanical strength of 63% for aligned scaffolds compared to 25% for randomly oriented scaffolds, despite similar overall amounts of collagen [130].

It can be hypothesized that cell shape changes induced by the nanofibrous structure lead to stimulation of ECM production. Several mechanisms may promote higher quantities of ECM deposition. There is evidence that cell maturation to a matrix-producing phenotype can be accelerated by aligned architecture. Collagen production of fibroblasts on aligned nanofiber substrate was 300% greater than on randomly oriented fibers at day 3, but was only 50% greater by day 7 [133]. Calcium production by bone marrow mesenchymal stem cells (BMSCs) was 50% higher at day 21, but not at days 4–14 [114]. It is also possible that cells are consistently stimulated to produce a greater amount of ECM, or that deposition increases could be a combination of both processes.

4.5 Cell Infiltration and Migration

Migration and infiltration of cells into tissue engineering scaffolds are crucial factors for their success. Many types of scaffold design require that cells seeded in vitro or recruited in vivo are allowed to infiltrate and populate the scaffolds quickly. Microstructure has a significant effect on cell migration and infiltration, and understanding these effects may lead to better scaffold design.

Random nanofibrous architecture has been observed to restrict cell migration as compared to flat controls [123, 136–138]. However, cell migration on nanofibrous substrates is greatly increased when the fibers are patterned in an aligned orientation. The number of cells migrating to a location 1.5 cm from their original seeding area was two to three times higher when aligned nanofibers guided cell migration as compared to random fibers or control film [123]. Cell migration into an in vitro wound defect model was increased by fivefold on substrates where aligned nanofibers were oriented toward the defect as compared to both randomly aligned fiber substrates or aligned fiber substrates oriented perpendicular to the defect (Fig. 9) [118]. Similarly, glioma cell migration velocity on aligned fibers was five times that seen on randomly oriented fiber substrates [139]. In addition, glioma stem cells containing neurospheres did not show cell detachment on random nanofiber substrates, but detached and migrated out on aligned nanofibers. Several factors could contribute to the migratory behavior of cells on nanofibrous substrates with different orientations: (1) Geometrical constraints may confine the random movement of cells on aligned nanofibers to one dimension, resulting in greater linear travel distances. (2) Cell morphologies and focal adhesion patterns modulated by the different types nanofibrous substrates may promote or hinder

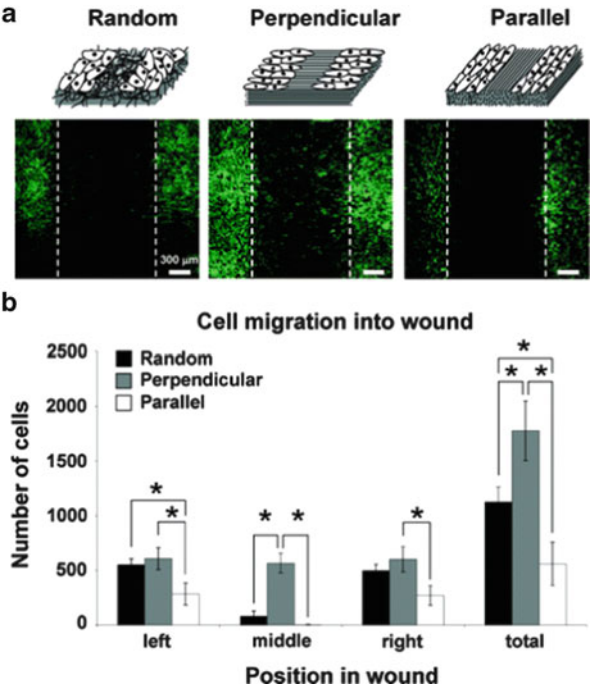

Fig. 9 (**a**) Dermal fibroblast migration into an in vitro wound healing model after 48 h on substrates with fibers aligned randomly, perpendicular to the defect or parallel to the defect. Cells are stained *green* for actin and *blue* for nuclei. *Dotted lines* are drawn at the initial edges of the wound. (**b**) Cell migration is quantified by the number of cells within the wound area divided equally into left, middle, and right zones. Statistically significant differences are marked with an *asterisk* [118]

cell migration [136, 139]. (3) Nanofibrous substrates may transduce cues through the cytoskeleton that encourage migratory or remodeling behaviors [122].

For regeneration of 3D tissue structures it is vital that tissue engineered scaffolds allow cell infiltration throughout their volume. The cell permeability of electrospun scaffolds with random orientation decreases with decreasing fiber size [140, 141], and small diameter scaffolds may completely exclude cell penetration. Fiber orientation can also have a significant effect on cell infiltration into nanofibrous scaffolds. In some cases, aligned orientations resulted in greater cell penetration as compared to randomly oriented scaffolds [142, 143]. In contrast, cell penetration has been observed into randomly aligned scaffolds, but not those with aligned orientations [115]. Similar cell infiltration into nanofibrous scaffolds with random and aligned orientation has also been observed [130]. There could be many factors involved in these discrepancies, such as fiber diameter, fiber mechanical properties, fiber-to-fiber adhesions, structural tensions on the fibers within the scaffold, and cell type preferences. Regardless of fiber orientation, cell penetration in nanofibrous scaffolds is generally limited and methods of addressing this limitation should be explored.

4.6 Differentiation and Gene Expression

In tissue engineering, it is crucial that cells introduced to a repair location differentiate into and/or maintain a desired phenotype. This is especially true when different

types of stem cells are intended to populate regenerating tissues. It is well established that different types of soluble cues can have strong effects on the differentiation of cells, but there is also strong evidence that structural features can be used to guide differentiation.

Although the effects of nanofibrous topography can be quite strong, its effects can be variable depending on cell types and specific experimental conditions. For example, one specific variable that can affect the differentiation induction of fibrous substrates is the diameter of the fibers [107]. Fibrous architecture has been observed to promote, prevent, and have no effect on differentiation as compared to a flat control for various cell types [106, 124, 138, 144]. This inconsistency might be due to the preferences of different cell types. It can be hypothesized that multipotent cells are directed to a phenotype that most closely corresponds to the morphology induced by the substrate that they are attached to. Accordingly, aligned nanofiber substrates have demonstrated the ability to promote differentiation of cells into several lineages that exhibit an elongated phenotype in vivo. BMSCs cultured on aligned nanofibers displayed ligament protein expression that suggested promotion of ligament phenotype maturation [59]. Tendon stem/progenitor cells expressed significantly higher amounts of tendon-specific genes when growing on aligned nanofibers compared to randomly oriented nanofibers in both normal and osteogenic media [145]. Several studies have observed myotube formation by skeletal muscle progenitor cells on aligned nanofiber substrates [146, 147]. The prevalence of nuclei contained in myotubes on aligned fibers has been quantified as up to 60% more than on randomly oriented fibers [52]. Primary cardiac ventricular cells also demonstrated development into a more mature phenotype when cultured on aligned nanofibers than on randomly oriented nanofibers, as confirmed by a threefold decrease in atrial natriuretic peptide expression [108]. Aligned architecture has a pronounced effect on neural differentiation and has been utilized to promote embryonic stem cell differentiation into neurons as opposed to astrocytes without the use of differentiation-inducing agents [148]. In agreement, embryonic stem cell differentiation into astrocytes on aligned nanofiber substrates was quantified as 33% less than on random fiber substrates [120]. Aligned nanofiber substrates also enhanced Schwann cell maturation compared to randomly oriented fibers, as indicated by upregulation of myelin-specific gene expression [109].

Cell differentiation is a complicated process and it is difficult to make a general hypothesis on the effect of surface topography on differentiation due to conflicting results and wide variations in specific experimental conditions. However, there is a significant amount of evidence indicating that aligned fibrous substrates promote differentiation into cellular phenotypes that exhibit an elongated morphology in vivo.

4.7 Mechanisms

Nanofibrous architecture presents a very different set of structural and biochemical cues to attached cells to that presented by flat culture surfaces. These variations

result in modulation of cell behaviors as the result of structural features. It can be theorized that three major mechanisms related to substrate structure are involved: (1) nutrient infiltration, (2) surface molecule presentation, and (3) cell shape-related mechanisms.

The 3D architecture of nanofibrous substrates may allow better nutrient exchange compared to flat surfaces because cells cultured on flat surfaces are limited to nutrient exchange on only one side. Specific nanofibrous orientations, such as aligned, can also offer different nutrient exchange potentials as compared to random orientations.

Nanofibrous substrates are also able to absorb greater amounts of protein and present surface biomolecules to cells very efficiently because of their high surface area-to-volume ratio. Studies have shown that nanofibrous substrates can absorb as much as 16 times more protein than flat surfaces, and increased protein absorption was related to specific changes in cell behavior between the two substrates [149, 150]. When a specific molecule is attached to a substrate to modulate cell behavior, the density of molecule presentation can be much higher in nanofibrous than in flat structures. Thus, biomolecule incorporation in nanofibers can lead to more efficient modulation of cell behaviors than other methods of presentation [151].

Cell shape has been shown to strongly influence cell behavior. The differentiation of MSCs was directed toward an osteoblastic fate when cells were allowed to flatten and spread, and were directed toward an adipogenic fate when constrained to a rounded shape [152]. Cytoskeletal organization, which is related to cell shape, could be the mechanism by which cell shape modulates other cell behaviors. In the previously described study, flattened or spread cells had more prominent stress fibers than rounded cells, and inhibition of myosin-generated cytoskeletal tension in those spread cells lead to adipogenic behaviors without changing cell shape [152]. In a similar study, differentiation of an adipogenic cell line was inhibited by allowing them to adopt a well-spread shape, but this inhibitory effect could be reversed by chemically disrupting the cytoskeleton [153]. The mechanism of transduction of cell shape and cytoskeletal properties into gene expression could be due to the transmission of mechanical forces from the cytoskeleton directly to the nucleus [154]. Nuclear shape has been directly measured and correlated with changes in gene expression and protein synthesis [155, 156]. Because aligned and randomly oriented nanofibrous substrates share similar dimensionality, it can be theorized that mechanisms related to cell shape are the major cause of cell behavior differences observed between the two substrates.

Topography-induced cell morphologies can be explained by cell receptor and membrane interactions with their underlying substrate. The elongated cell morphology commonly observed on aligned nanofiber substrates may be regulated by receptor adhesion characteristics and cell membrane configurations associated with nanofiber structure and orientation. Nanofibrous topography could be a key factor for activation of adhesion proteins and integrin expression, and the specific orientation and diameter of nanofibrous substrates can result in significant effects on overall expression and distribution patterns of integrin receptors [132, 134, 145]. Integrin receptor expression was up to 15 times greater in cells attached to aligned

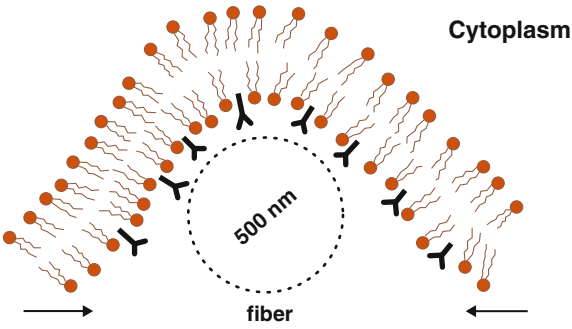

Fig. 10 Cell membrane wrapping around a nanofiber with compatible ligands. *Arrows* indicate membrane wrapping to reduce free energy of the interaction and increase the local curvature of the membrane [116]

nanofiber substrates compared to those with random orientation [145]. In addition, the location and orientation of filament structures protruding out of cells was different on aligned and randomly oriented nanofiber structures [117, 145]. The geometry of nanofibers may also lead to interactions with the cell membrane that result in an elongated structure. When a cell comes in contact with a fiber, its membrane receptors bind to ligands on the fiber surface and the membrane wraps around the fiber to reduce the free energy of the reaction (Fig. 10) [116]. This results in increased elastic energy, associated with increased curvature of the membrane, which is reduced as the cell elongates along the fiber [116].

5 Tissue Engineering Applications

Aligned nanofibrous structures have many applications in the biomedical field, including sutures [46, 157] and drug delivery applications [46]. However, one of the most promising uses for these aligned structures is in tissue engineering constructs applications and tissue regeneration. As previously mentioned, tissues such as nerve, blood vessel, skeletal muscle, and bone contain highly aligned collagen fibrils or other aligned protein nanofibers. This precisely arranged structure is very important in order to provide the necessary properties for these tissues to serve their intended function. When these tissues become injured or degenerated, intervention must take place to restore function. Regeneration of aligned tissue using an aligned nanofiber tissue engineering approach has been investigated in tissue types including, but not limited to, neural [109, 117, 158–163], vascular [87, 131, 164–170], skeletal muscle [52, 110], bone [58, 114, 171–175], cartilage [111, 130, 176–180], ligament [104, 123, 181], and tendon [145, 175]. This research area focuses on fabricating highly aligned natural or synthetic polymer nanofiber structures in order to serve as a matrix for cells to regenerate aligned tissue with structures similar to native tissue. Evidence presented in Sect. 4 leads to the hypothesis that regeneration of aligned tissues will be more effective when the native structure is mimicked as closely as possible. The synthetic scaffold serves as a template for the cells to attach to and align on, and also promotes newly produced

ECM to align. Researchers are now using this approach to attempt to regenerate a wide variety of aligned tissues. Such approaches are summarized below, with a focus on the most advanced, clinically related translational approaches.

5.1 Neural Tissue

Neural tissue regeneration is one of the most commonly investigated applications of aligned nanofiber-based tissue engineering constructs. The most clinically relevant studies are related to peripheral nerve regeneration through the use of nerve conduits after injury or degeneration. The ability of nerves to regenerate and restore function depends on the alignment and elongation of healthy neurites across an injury site to reestablish connections. Though the peripheral nervous system has a natural regenerative capacity, surgical intervention may be necessary to stimulate axonal growth across the damaged nerve gap in order to restore function, especially in more serious injuries. Current methods to accomplish this include the use of allografts or autografts; however, there are many issues associated with these methods, including limited availability. A common tissue engineering approach to stimulate nerve regeneration is the implantation of a semipermeable nerve conduit that connects two nerve stumps. These conduits allow the free exchange of nutrients and growth factors required for nerve regeneration while providing a protected growth environment. Recently, the use of aligned nanofibers in nerve conduits has generated a lot of interest due to their ability to promote alignment and elongation in regenerating axons, and preferential differentiation of neural stem cells into neurons. In natural peripheral nerve regeneration, axon regrowth is guided by aligned ECM proteins [2]. Aligned nanofiber substrates may be able to fill this role in tissue engineering approaches.

Nanofibrous architecture has been incorporated into nerve conduits in several configurations. Electrospinning is the preferred method of nanofiber fabrication for these scaffolds due to its versatility and its capacity to produce long aligned fibers (of several centimeters) that completely span the nerve gap. Nerve conduits may be fabricated entirely from aligned nanofibers or they may be attached to the inner surface of a nerve conduit made from another material. Single material nanofiber conduits can be manufactured by rolling flat aligned nanofiber sheets into a tubular structure (Fig. 11), but modified one-step electrospinning methods have also been

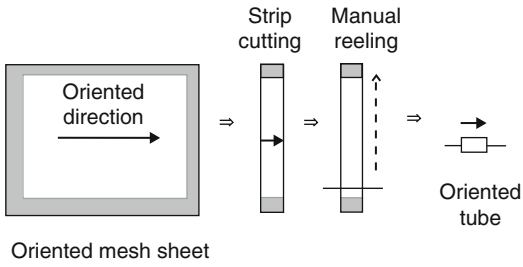

Fig. 11 3D construction of nerve conduit by rolling a sheet of aligned nanofibers [192]

developed to form tubular structures with axial nanofiber alignment [82]. Composite nerve guidance tubes containing axially aligned nanofibers attached to their inner walls can be fabricated when polymer films are coated with aligned nanofibers and rolled into a tubular structure [119, 159].

Nerve conduits have been evaluated in nerve defect models, such as the sciatic nerve, in order to evaluate their capacity to promote nerve tissue regeneration [159]. The results of several such studies have demonstrated significantly enhanced nerve regeneration for conduits containing aligned nanofibers, as compared to controls without fibers. For instance, a 15 mm critical defect gap was effectively bridged in 100% of the rats treated with rolled polymer film conduits coated with aligned nanofibers, whereas controls, without nanofibers, only bridged the gap in 50% of the rats [159]. Both axially and circumferentially aligned nanofibers promoted a significant increase in nerve cross-sectional area compared to controls, but grafts with axial nanofiber alignment promoted more myelinated axons and a higher percentage of electrophysiological recovery than grafts with circumferentially aligned fibers [159]. While these results are promising, aligned nanofibers were only present on the inner walls of these conduits, and thus only neurons regenerating near the walls of the grafts had direct contact with the nanofibrous architecture. Other methods have been developed to distribute aligned nanofibers throughout the volume of a nerve bridging conduit. Flat nanofiber-containing sheets rolled into spiral shapes [115, 158] provide some aligned fiber structure throughout the graft volume. Micrometer diameter nanofiber yarns were also inserted into bridging conduits to distribute nanofibrous structure throughout their full thickness [163]. In some cases, nerve conduits containing aligned nanofiber yarns performed better than nerve autografts in promoting recovery of sensory and motor function after sciatic nerve resection [163]. Growth factor incorporation, such as nerve growth factor and glial cell-derived neurotrophic factor, can further improve the performance of nerve bridging conduits containing aligned nanofibers [159, 163].

Similar neural applications of aligned nanofibers include spinal cord repair and regeneration of aligned neural tracks in the brain. These applications, however, are much more difficult to address due to the increased inflammatory response in CNS tissue, as well as the lack of natural regeneration in CNS tissues.

5.2 Vascular Tissue

Aligned nanofibrous scaffolds are also being investigated as tissue engineering solutions for disease and degeneration in cardiovascular tissues [87, 165, 167, 168]. Aligned nanofibers could have several cardiovascular system applications, such as cardiac patches [43, 108], but the main thrust of research in this area is in the design of a vascular graft. The prevalence of vascular and heart disease is extremely high, with many of these problems arising from occlusions in coronary and peripheral arteries. Autologous grafting procedures are limited by a lack of donor tissue and by patient morbidity associated with harvest surgery. Current prosthetic grafts

suffer from low patency rates due to issues arising from thrombosis, compliance mismatch, and biocompatibility. It is apparent that a better graft is needed, and aligned nanofibers offer several attractive properties for vascular graft design. Aligned nanofibers may be used to direct smooth muscle cell arrangement in a circumferentially aligned orientation similar to natural vessels and could promote ordered ECM assembly in this configuration. In addition, aligned nanofibers can offer excellent mechanical strength. Tensile strength increases with increasing degree of fiber alignment, which is extremely important in resisting the high pressures associated with this application [182].

Similar to nerve conduits, vascular grafts can be fabricated by rolling flat aligned electrospun nanofibrous sheets into tubular constructs [87]. Fiber sheets are rolled in a way that aligns fibers in the circumferential direction in order to provide mechanical strength and circumferential cell guidance specific to vascular tissue. Fully cellularized grafts may be fabricated when cells are grown on aligned nanofiber sheets before rolling into a tubular structure [168]. Such fully cellularized grafts showed promising results after 60 days in vivo [168]. The cellular morphology and orientation of the ECM produced in the grafts were very similar to that of the native ECM, perhaps in part due to the aligned nanofiber microstructure.

One-step fabrication of tubular grafts directly on a rotating mandrel is desirable to improve efficiency, as well as to ensure a uniform structure with adhesion between layers and no line of weakness. Randomly oriented tubular vascular grafts are commonly fabricated in one step using the rotating mandrel electrospinning method. However, this method alone is not sufficient for the fabrication of a small diameter graft with circumferential fiber alignment. Fiber alignment is dependent on matching the electrospinning jet speed with the tangential velocity of the collecting mandrel, and the tangential velocity of the mandrel is dependent on both the rotational velocity and the collection mandrel diameter (tangential velocity = rotational velocity × mandrel diameter × π). Therefore, when a small mandrel of a few millimeters is used, the required rotational velocities become so high that ordered collection is disrupted. However, a small diameter tubular graft with aligned fibers has been fabricated directly on a rotating mandrel using a modified collection method, as described in Sect. 3.3.1 (Fig. 5). In this case, the path of the electrospinning jet was controlled by oppositely charged electrodes, and a nonconductive rotating mandrel was placed between the spinneret and the electrodes to collect nanofibers. This method allowed the fabrication of well-aligned nanofiber tubes with controlled fiber angles, which were collected on mandrels as small as 4 mm at rotational speeds less than 1,000 rpm [87].

5.3 Skeletal Muscle

Skeletal muscle tissue engineering requires a considerably different structure than the two other tissues discussed above. The main concern with skeletal muscle regeneration is the alignment and maturation of large multinucleated muscle fibers.

This is especially important because it affects the ability of the muscle to contract as a whole. For this reason, an aligned nanofibrous tissue engineering approach is being investigated for skeletal muscle regeneration [52, 110, 146]. The focus in regenerating this tissue is to promote the development of full-thickness skeletal muscle grafts that can be implanted in variously shaped skeletal muscle defects caused by congenital conditions, traumatic injury, and tumor excision. Such grafts should promote the in vivo development of a 3D extracellular matrix and fully functional vascularized multinucleated muscle fibers. Current research, however, is still generally focused on 2D nanofiber scaffolds. Progenitor cell lines such as C2C12 myoblasts or explanted skeletal muscle cells are most often seeded onto highly aligned nanofibrous sheets to determine the ability of the aligned scaffolds to guide cellular alignment and myotube formation [52, 110]. Results indicate that cells seeded onto aligned nanofibrous scaffolds exhibit significantly greater alignment, myotube formation, and myotube contractility, as indicated by correctly arranged sarcomeric contractile machinery [52, 110]. Challenges in utilizing aligned nanofibers in skeletal muscle tissue engineering include the design of structures that promote alignment and myotube maturation in 3D, while promoting the vascularization that is required for sustaining cell survival and function within thicker constructs.

5.4 Bone

Bone is another tissue investigated for aligned nanofibrous tissue regeneration strategies. With bone disease and defects being extremely prevalent in today's active and aging population, the need for bone substitutes is very high. Current strategies for treating critically sized defects in bone include allografts and autografts; however, these methods have many issues, including lack of available donors, donor site morbidity [183], and infection [184]. For these reasons, researchers are investigating a regenerative approach when trying to solve this problem. With the structure and composition of bone consisting of hydroxyapatite deposited on highly aligned collagen fibers, it makes sense that aligned nanofibers are now being investigated as scaffolds for the regeneration of bone tissue. Aligned nanofiber scaffolds can provide mechanical strength and promote cellular alignment and ordered ECM production. In addition, hydroxyapatite can be coated onto these aligned nanofibers, or incorporated within, in order to from a bonelike composite structure [185, 186]. From here, strategies could be developed to create numerous different types of 3D structures, incorporating aligned nanofibers, which may allow the regeneration of multiple types and structures of bone.

5.5 Cartilage, Tendons and Ligaments

Aligned nanofiber-based approaches are also being investigated for regeneration of connective tissue such as cartilage, tendons, and ligaments. Aligned collagen fibrils,

found in the superficial zone of articular cartilage, provide crucial tensile strength to the tissue. Degeneration of the collagen in this zone, due to osteoarthritis, aging, and injury, often results in significantly diminished mechanical properties of the cartilage. Tissue engineering approaches are being investigated as methods to regenerate the superficial zone of articular cartilage to restore function [111, 130]. MSCs cultured on aligned nanofiber substrates have demonstrated enhanced chondrogenic differentiation and deposited a well organized ECM that had significantly greater mechanical strength than unorganized ECM deposited on non-aligned nanofiber substrates [111, 130].

Aligned nanofibrous scaffolds are also well suited for the regeneration of ligaments and tendons because they mimic the tightly packed aligned collagen fibrils that are a major component of these tissues. Explanted tendon and ligament cells have been cultured on aligned nanofibers and in aligned nanofiber/hydrogel composite substrates to evaluate their potential as tissue engineering scaffolds [104, 112]. However, similar to bone and skeletal muscle regeneration, research in aligned fiber-based regeneration of cartilage, tendon, and ligament tissue is generally limited to in vitro responses of tissue-specific cells to aligned nanofibrous substrates.

Directly after implantation, tendon and ligament scaffolds would have to withstand the large forces that these tissues experience daily. For this reason, tissue scaffolds must be both mechanically strong and promote tissue regeneration. Aligned nanofibrous scaffolds in yarn-like structures may be suitable for mimicking the natural structure of these tissues and enhancing the mechanical properties. Several techniques have been investigated to fabricate nonwoven and braided yarn-like structures from aligned nanofibers [45, 187, 188].

5.6 Cornea

Other less conventional tissues are also being investigated using an aligned nanofibrous tissue engineering approach, including the cornea. The very distinct structure of the cornea creates a transparent membrane that is minimally disruptive to the passage of light, for enhanced vision. This structure is composed of proteoglycans and highly aligned collagen I and collagen IV fibers, which are of uniform diameter and uniformly spaced apart. These aligned protein nanofibers are formed into lamellae and can be stacked at varying angles [68, 189]. Tissue engineering approaches are now being considered as a potential treatment for corneal blindness. Preliminary data indicate that a tissue engineering scaffold fabricated by electrospinning collagen I is a promising method for cornea tissue regeneration [68, 189].

5.7 Challenges

Nanofiber-based tissue engineering strategies are faced with similar challenges to those encountered throughout the field of tissue engineering. These challenges

include selection and design of materials that are bioactive and possess suitable mechanical properties, as well as optimized degradation rates. In addition, scaffolds must be designed in a way that allows cell infiltration throughout their volume and promotes functional vascular formation to sustain cellular ingrowth.

Great advances are constantly being made in the design of new biomaterials and the identification of functional molecules that produce desirable cell responses. However, it can be difficult to apply these advances to aligned nanofibrous-based tissue engineering strategies due to fabrication constraints, such as specific solubility and electrical property requirements as well as thermal or chemical biomolecule deactivation. The major materials-related challenges in aligned nanofibrous scaffold fabrication are generally related to developing methods to fabricate aligned nanofibers from the most desirable materials and finding ways to incorporate the most desirable functional molecules. In addition, the unique structure of aligned nanofibers can have a pronounced effect on material properties such as mechanical strength and degradation rate, and on cell interactions with surface molecules.

The second major challenge in aligned nanofiber tissue engineering is in assembling the fibers into 3D structures with an architecture that is permeable to cell infiltration and vascular ingrowth. Aligned nanofibers in a 3D bundle or stack tend to be tightly packed together and thus offer little room for cell infiltration. Methods of fabricating 3D aligned nanofiber structures with a loose structure or controlled packing density must be developed to improve the cell penetration properties of these scaffolds. Examples of strategies to address this problem include incorporating a sacrificial fiber component into an aligned nanofiber mat [190], and fabrication of a composite material in which aligned nanofibers are fixed in a cell-permeable substrate at a controlled packing density [191].

6 Concluding Remarks

Many tissues rely on a well-aligned cellular and ECM orientation to perform their required functions. Damage and degeneration of these tissues requires a regenerative response that restores function. It is hypothesized that tissue engineering approaches that restore similar cellular morphology and structural architectures result in better functional recovery. It has been shown in vitro that cell behaviors such as morphology, elongation, proliferation, ECM production, and differentiation can all be modulated by scaffold architecture. Furthermore, aligned substrates, such as aligned polymer nanofibers, promote cell behaviors associated with aligned tissues. Behaviors desirable in aligned tissue engineering include elongation, unidirectional alignment, ordered ECM production, accelerated unidirectional migration, and preferred differentiation of stem cells into phenotypes associated with aligned tissues. Despite the promise of aligned polymer nanofibers, functional in vivo tissue engineering strategies are somewhat limited due to difficulties in assembling aligned nanofiber scaffolds with precisely controlled architecture. This is especially relevant for 3D scaffolds required for regeneration of thick

vascularized tissues. Researchers are currently exploring better and more versatile ways to fabricate electrospun aligned nanofibers and assemble them into structures. Such techniques increased fiber alignment, length, and yield, and allowed more precise control of fiber deposition location, fiber density, and fiber orientation within aligned nanofiber structures. We hypothesize that the potential of aligned polymer nanofibers in the clinical setting will be realized as innovative methods of aligned nanofiber assembly are applied to the design of better, more precisely assembled functional tissue engineering scaffolds.

Acknowledgment This work is supported by the grants from NIH (NS050243), NIH/NCRR (P20RR021949), and American Heart Association.

References

1. Sakai T, Larsen M, Yamada KM (2003) Fibronectin requirement in branching morphogenesis. Nature 423(6942):876–881
2. Fawcett JW, Keynes RJ (1990) Peripheral nerve regeneration. Annu Rev Neurosci 13:43–60
3. Rebustini IT et al (2007) Laminin alpha5 is necessary for submandibular gland epithelial morphogenesis and influences FGFR expression through beta1 integrin signaling. Dev Biol 308(1):15–29
4. Beachley V, Wen X (2010) Polymer nanofibrous structures: fabrication, biofunctionalization, and cell interactions. Prog Polym Sci 35(7):868–892
5. Huang Z-M et al (2003) A review on polymer nanofibers by electrospinning and their applications in nanocomposites. Compos Sci Technol 63(15):2223–2253
6. Jeong HE et al (2006) Stretched polymer nanohairs by nanodrawing. Nano Lett 6 (7):1508–1513
7. Xing X, Wang Y, Li B (2008) Nanofibers drawing and nanodevices assembly in poly (trimethylene terephthalate). Opt Express 16(14):10815–10822
8. Nain A et al (2006) Drawing suspended polyer micro-/nanofibers using glass micropipettes. Appl Phys Lett 89:1831051–1831053
9. Nain AS et al (2009) Dry spinning based spinneret based tunable engineered parameters (STEP) technique for controlled and aligned deposition of polymeric nanofibers. Macromol Rapid Commun 30(16):1406–1412
10. Cheng F et al (2006) Conducting poly(aniline) nanotubes and nanofibers: controlled synthesis and application in lithium/poly(aniline) rechargeable batteries. Chemistry 12(11):3082–3088
11. Badrossamay MR et al (2010) Nanofiber assembly by rotary jet-spinning. Nano Lett 10 (6):2257–2261
12. Li HY, Ke YC, Hu YL (2006) Polymer nanofibers prepared by template melt extrusion. J Appl Polym Sci 99(3):1018–1023
13. Grimm S et al (2008) Nondestructive replication of self-ordered nanoporous alumina membranes via cross-linked polyacrylate nanofiber arrays. Nano Lett 8(7):1954–1959
14. Porter JR, Henson A, Popat KC (2009) Biodegradable poly(epsilon-caprolactone) nanowires for bone tissue engineering applications. Biomaterials 30(5):780–788
15. Lee W et al (2004) Nanostructuring of a polymeric substrate with well-defined nanometer-scale topography and tailored surface wettability. Langmuir 20(18):7665–7669
16. Tao SL, Desai TA (2007) Aligned arrays of biodegradable poly(epsilon-caprolactone) nanowires and nanofibers by template synthesis. Nano Lett 7(6):1463–1468
17. Sheng XL, Zhang JH (2009) Superhydrophobic behaviors of polymeric surfaces with aligned nanofibers. Langmuir 25(12):6916–6922

18. Prasanthkumar S et al (2010) Solution phase epitaxial self-assembly and high charge-carrier mobility nanofibers of semiconducting molecular gelators. J Am Chem Soc 132(26):8866–8867
19. Weronski KJ et al (2010) Time-lapse atomic force microscopy observations of the morphology, growth rate, and spontaneous alignment of nanofibers containing a peptide-amphiphile from the hepatitis G virus (NS3 protein). J Phys Chem B 114(1):620–625
20. Hung AM, Stupp SI (2009) Understanding factors affecting alignment of self-assembling nanofibers patterned by sonication-assisted solution embossing. Langmuir 25(12):7084–7089
21. Hung AM, Stupp SI (2007) Simultaneous self-assembly, orientation, and patterning of peptide-amphiphile nanofibers by soft lithography. Nano Lett 7(5):1165–1171
22. Nogueira GM et al (2010) Layer-by-layer deposited chitosan/silk fibroin thin films with anisotropic nanofiber alignment. Langmuir 26(11):8953–8958
23. Kyotani M et al (2010) Entanglement-free fibrils of aligned polyacetylene films that produce single nanofibers. Nanoscale 2(4):509–514
24. Mata A et al (2009) Micropatterning of bioactive self-assembling gels. Soft Matter 5 (6):1228–1236
25. Everett TA, Higgins DA (2009) Electrostatic self-assembly of ordered perylene-diimide/polyelectrolyte nanofibers in fluidic devices: from nematic domains to macroscopic alignment. Langmuir 25(22):13045–13051
26. Merzlyak A, Indrakanti S, Lee SW (2009) Genetically engineered nanofiber-like viruses for tissue regenerating materials. Nano Lett 9(2):846–852
27. Lee P et al (2006) Microfluidic alignment of collagen fibers for in vitro cell culture. Biomed Microdevices 8(1):35–41
28. Guo Y et al (2006) Alignment of glycolipid nanotubes on a planar glass substrate using a two-step microextrusion technique. J Nanosci Nanotechnol 6(5):1464–1466
29. Kim J et al (2008) Magnetic field effect for cellulose nanofiber alignment. J Appl Phys 104 (9):096104
30. Sugiyama J, Chanzy H, Maret G (1992) Orientation of cellulose microcrystals by strong magnetic fields. Macromolecules 25(16):4232–4234
31. Torbet J, Ronziere MC (1984) Magnetic alignment of collagen during self-assembly. Biochem J 219:1057–1059
32. Lowik D et al (2007) A highly ordered material from magnetically aligned peptide amphiphile nanofiber assemblies. Adv Mater 19(9):1191−+
33. Guo C, Kaufman LJ (2007) Flow and magnetic field induced collagen alignment. Biomaterials 28(6):1105–1114
34. Rollings DA et al (2007) Formation and aqueous surface wettability of polysiloxane nanofibers prepared via surface initiated, vapor-phase polymerization of organotrichlorosilanes. Langmuir 23(10):5275–5278
35. Sun QH et al (2009) Fabrication of aligned polyaniline nanofiber array via a facile wet chemical process. Macromol Rapid Commun 30(12):1027–1032
36. Li M, Wei ZX, Jiang L (2008) Polypyrrole nanofiber arrays synthesized by a biphasic electrochemical strategy. J Mater Chem 18(19):2276–2280
37. Czaja WK et al (2007) The future prospects of microbial cellulose in biomedical applications. Biomacromolecules 8(1):1–12
38. Kondo T et al (2002) Biodirected epitaxial nanodeposition of polymers on oriented macromolecular templates. Proc Natl Acad Sci USA 99(22):14008–14013
39. Putra A et al (2008) Tubular bacterial cellulose gel with oriented fibrils on the curved surface. Polymer 49(7):1885–1891
40. Uraki Y et al (2007) Honeycomb-like architecture produced by living bacteria, gluconacetobacter xylinus. Carbohydr Polym 69(1):1–6
41. Sano MB et al (2010) Electromagnetically controlled biological assembly of aligned bacterial cellulose nanofibers. Ann Biomed Eng 38(8):2475–2484
42. Afifi AM et al (2009) Fabrication of aligned poly(L-lactide) fibers by electrospinning and drawing. Macromol Mater Eng 294(10):658–665

43. Zong X et al (2005) Electrospun fine-textured scaffolds for heart tissue constructs. Biomaterials 26(26):5330–5338
44. Ji JY et al (2009) Significant improvement of mechanical properties observed in highly aligned carbon-nanotube-reinforced nanofibers. J Phys Chem C 113(12):4779–4785
45. Smit E, Buttner U, Sanderson RD (2005) Continuous yarns from electrospun fibers. Polymer 46(8):2419–2423
46. Reneker DH, Chun I (1996) Nanometre diameter fibres of polymer, produced by electrospinning. Nanotechnology 7(3):216–223
47. Yee WA et al (2007) Morphology, polymorphism behavior and molecular orientation of electrospun poly(vinylidene fluoride) fibers. Polymer 48(2):512–521
48. Wu YQ, Carnell LA, Clark RL (2007) Control of electrospun mat width through the use of parallel auxiliary electrodes. Polymer 48(19):5653–5661
49. Edwards MD et al (2010) Development of orientation during electrospinning of fibres of poly (epsilon-caprolactone). Eur Polym J 46(6):1175–1183
50. Bashur CA, Dahlgren LA, Goldstein AS (2006) Effect of fiber diameter and orientation on fibroblast morphology and proliferation on electrospun poly(D, L-lactic-co-glycolic acid) meshes. Biomaterials 27(33):5681–5688
51. Wang HB et al (2009) Creation of highly aligned electrospun poly-L-lactic acid fibers for nerve regeneration applications. J Neural Eng 6(1):016001
52. Aviss KJ, Gough JE, Downes S (2010) Aligned electrospun polymer fibres for skeletal muscle regeneration. Eur Cells Mater 19:193–204
53. Courtney T et al (2006) Design and analysis of tissue engineering scaffolds that mimic soft tissue mechanical anisotropy. Biomaterials 27(19):3631–3638
54. Zhong S et al (2006) An aligned nanofibrous collagen scaffold by electrospinning and its effects on in vitro fibroblast culture. J Biomed Mater Res A 79(3):456–463
55. Lee JY et al (2010) Enhanced polarization of embryonic hippocampal neurons on micron scale electrospun fibers. J Biomed Mater Res A 92A(4):1398–1406
56. Li WJ et al (2007) Engineering controllable anisotropy in electrospun biodegradable nanofibrous scaffolds for musculoskeletal tissue engineering. J Biomech 40(8): 1686–1693
57. Chan KHK et al (2010) Morphologies and electrical properties of electrospun poly (R)-3-hydroxybutyrate-co-(R)-3-hydroxyvalerate/multiwalled carbon nanotubes fibers. J Appl Polym Sci 116(2):1030–1035
58. Thomas V et al (2006) Mechano-morphological studies of aligned nanofibrous scaffolds of polycaprolactone fabricated by electrospinning. J Biomater Sci Polym Ed 17(9):969–984
59. Bashur CA et al (2009) Effect of fiber diameter and alignment of electrospun polyurethane meshes on mesenchymal progenitor cells. Tissue Eng A 15(9):2435–2445
60. McClure MJ et al (2009) Electrospinning-aligned and random polydioxanone-polycaprolactone-silk fibroin-blended scaffolds: geometry for a vascular matrix. Biomed Mater 4(5):055010
61. Jose MV et al (2007) Morphology and mechanical properties of Nylon 6/MWNT nanofibers. Polymer 48(4):1096–1104
62. Li D, Wang YL, Xia YN (2003) Electrospinning of polymeric and ceramic nanofibers as uniaxially aligned arrays. Nano Lett 3(8):1167–1171
63. Xin Y et al (2008) Fabrication of well-aligned PPV/PVP nanofibers by electrospinning. Mater Lett 62(6–7):991–993
64. Kuo CC, Wang CT, Chen WC (2008) Highly-aligned electrospun luminescent nanofibers prepared from polyfluorene/PMMA blends: fabrication, morphology, photophysical properties and sensory applications. Macromol Mater Eng 293(12):999–1008
65. Dalton PD et al (2007) Electrospinning of polymer melts: phenomenological observations. Polymer 48(23):6823–6833
66. Jalili R et al (2006) Fundamental parameters affecting electrospinning of PAN nanofibers as uniaxially aligned fibers. J Appl Polym Sci 101(6):4350–4357

67. Li D, Wang YL, Xia YN (2004) Electrospinning nanofibers as uniaxially aligned arrays and layer-by-layer stacked films. Adv Mater 16(4):361–366
68. Wray LS, Orwin EJ (2009) Recreating the microenvironment of the native cornea for tissue engineering applications. Tissue Eng A 15(7):1463–1472
69. Bazbouz MB, Stylios GK (2008) Alignment and optimization of nylon 6 nanofibers by electrospinning. J Appl Polym Sci 107(5):3023–3032
70. Liu LH, Dzenis YA (2008) Analysis of the effects of the residual charge and gap size on electrospun nanofiber alignment in a gap method. Nanotechnology 19(35):355307
71. Katta P et al (2004) Continuous electrospinning of aligned polymer nanofibers onto a wire drum collector. Nano Lett 4(11):2215–2218
72. Teo WE, Ramakrishna S (2006) A review on electrospinning design and nanofibre assemblies. Nanotechnology 17:R89–R106
73. Pokorny M, Niedoba K, Velebny V (2010) Transversal electrostatic strength of patterned collector affecting alignment of electrospun nanofibers. Appl Phys Lett 96(19):193111
74. Beachley V, Wen X (2009) Effect of electrospinning parameters on the nanofiber diameter and length. Mater Sci Eng C 29:663–668
75. Teo WE, Ramakrishna S (2005) Electrospun fibre bundle made of aligned nanofibres over two fixed points. Nanotechnology 16(9):1878–1884
76. Ayutsede J et al (2006) Carbon nanotube reinforced Bombyx mori silk nanofibers by the electrospinning process. Biomacromolecules 7(1):208–214
77. Carnell LS et al (2009) Electric field effects on fiber alignment using an auxiliary electrode during electrospinning. Scr Mater 60(6):359–361
78. Acharya M, Arumugam GK, Heiden PA (2008) Dual electric field induced alignment of electrospun nanofibers. Macromol Mater Eng 293(8):666–674
79. Kim G, Kim W (2006) Formation of oriented nanofibers using electrospinning. Appl Phys Lett 88:233101
80. Deitzel JM et al (2001) Controlled deposition of electrospun poly(ethylene oxide) fibers. Polymer 42:8163–8170
81. Theron A, Zussman E, Yarin AL (2001) Electrostatic field-assisted alignment of electrospun nanofibres. Nanotechnology 12(3):384–390
82. Yao L et al (2009) Orienting neurite growth in electrospun fibrous neural conduits. J Biomed Mater Res B Appl Biomater 90B(2):483–491
83. Bhattarai N et al (2005) Electrospun chitosan-based nanofibers and their cellular compatibility. Biomaterials 26(31):6176–6184
84. Secasanu VP, Giardina CK, Wang YD (2009) A novel electrospinning target to improve the yield of uniaxially aligned fibers. Biotechnol Prog 25(4):1169–1175
85. Carnell LS et al (2008) Aligned mats from electrospun single fibers. Macromolecules 41 (14):5345–5349
86. Sundaray B et al (2004) Electrospinning of continuous aligned polymer fibers. Appl Phys Lett 84(7):1222–1224
87. Teo WE et al (2005) Porous tubular structures with controlled fibre orientation using a modified electrospinning method. Nanotechnology 16(6):918–924
88. Mo XM, Weber HJ (2004) Electrospinning P(LLA-CL) nanofiber: a tubular scaffold fabrication with circumferential alignment. Macromol Symp 217:413–416
89. Lee H, Yoon H, Kim G (2009) Highly oriented electrospun polycaprolactone micro/nanofibers prepared by a field-controllable electrode and rotating collector. Appl Phys A Mater Sci Process 97(3):559–565
90. Kim GH (2006) Electrospinning process using field-controllable electrodes. J Polym Sci B Polym Phys 44(10):1426–1433
91. Attout A, Yunus S, Bertrand P (2008) Electrospinning and alignment of polyaniline-based nanowires and nanotubes. Polym Eng Sci 48(9):1661–1666
92. Ishii Y, Sakai H, Murata H (2008) A new electrospinning method to control the number and a diameter of uniaxially aligned polymer fibers. Mater Lett 62(19):3370–3372

93. Kessick R, Fenn J, Tepper G (2004) The use of AC potentials in electrospraying and electrospinning processes. Polymer 45(9):2981–2984
94. Sarkar S, Deevi S, Tepper G (2007) Biased AC electrospinning of aligned polymer nanofibers. Macromol Rapid Commun 28(9):1034–1039
95. Rafique J et al (2007) Electrospinning highly aligned long polymer nanofibers on large scale by using a tip collector. Appl Phys Lett 91:063126
96. Zhou W et al (2007) Gas flow-assisted alignment of super long electrospun nanofibers. J Nanosci Nanotechnol 7(8):2667–2673
97. Liu YQ et al (2010) Magnetic-field-assisted electrospinning of aligned straight and wavy polymeric nanofibers. Adv Mater 22(22): 2454−+
98. Beachley V, Wen X (2010) Fabrication of three dimensional aligned nanofiber array, *US-7828539*, Clemson University (Clemson, SC, US) US
99. Madhugiri S et al (2003) Electrospun MEH-PPV/SBA-15 composite nanofibers using a dual syringe method. J Am Chem Soc 125(47):14531–14538
100. Kidoaki S, Kwon IK, Matsuda T (2005) Mesoscopic spatial designs of nano- and microfiber meshes for tissue-engineering matrix and scaffold based on newly devised multilayering and mixing electrospinning techniques. Biomaterials 26(1):37–46
101. Ding B et al (2004) Fabrication of blend biodegradable nanofibrous nonwoven mats via multi-jet electrospinning. Polymer 45(6):1895–1902
102. Theron SA et al (2005) Multiple jets in electrospinning: experiment and modeling. Polymer 46(9):2889–2899
103. Chow WN et al (2007) Evaluating neuronal and glial growth on electrospun polarized matrices: bridging the gap in percussive spinal cord injuries. Neuron Glia Biol 3:119–126
104. Hayami JWS et al (2010) Design and characterization of a biodegradable composite scaffold for ligament tissue engineering. J Biomed Mater Res A 92A(4):1407–1420
105. Yao YF et al (2007) Fiber-oriented liquid crystal polarizers based on anisotropic electrospinning. Adv Mater 19(21): 3707−+
106. Li WJ et al (2003) Biological response of chondrocytes cultured in three-dimensional nanofibrous poly(epsilon-caprolactone) scaffolds. J Biomed Mater Res A 67(4):1105–1114
107. Yang F et al (2005) Electrospinning of nano/micro scale poly(L-lactic acid) aligned fibers and their potential in neural tissue engineering. Biomaterials 26(15):2603–2610
108. Rockwood DN et al (2008) Culture on electrospun polyurethane scaffolds decreases atrial natriuretic peptide expression by cardiomyocytes in vitro. Biomaterials 29(36):4783–4791
109. Chew SY et al (2008) The effect of the alignment of electrospun fibrous scaffolds on Schwann cell maturation. Biomaterials 29(6):653–661
110. Choi JS et al (2008) The influence of electrospun aligned poly(epsilon-caprolactone)/collagen nanofiber meshes on the formation of self-aligned skeletal muscle myotubes. Biomaterials 29(19):2899–2906
111. Wise JK et al (2009) Chondrogenic differentiation of human mesenchymal stem cells on oriented nanofibrous scaffolds: engineering the superficial zone of articular cartilage. Tissue Eng A 15(4):913–921
112. Moffat KL et al (2009) Novel nanofiber-based scaffold for rotator cuff repair and augmentation. Tissue Eng A 15(1):115–126
113. Corey JM et al (2007) Aligned electrospun nanofibers specify the direction of dorsal root ganglia neurite growth. J Biomed Mater Res A 83A(3):636–645
114. Ma J, He X, Jabbari E (2011) Osteogenic differentiation of marrow stromal cells on random and aligned electrospun poly(l-lactide) nanofibers. Ann Biomed Eng 39:14–25
115. Nisbet DR et al (2009) Neurite infiltration and cellular response to electrospun polycaprolactone scaffolds implanted into the brain. Biomaterials 30(27):4573–4580
116. Tian F et al (2008) Quantitative analysis of cell adhesion on aligned micro- and nanofibers. J Biomed Mater Res A 84(2):291–299
117. He LM et al (2010) Synergistic effects of electrospun PLLA fiber dimension and pattern on neonatal mouse cerebellum C17.2 stem cells. Acta Biomater 6(8):2960–2969

118. Patel S et al (2007) Bioactive nanofibers: synergistic effects of nanotopography and chemical signaling on cell guidance. Nano Lett 7(7):2122–2128
119. Madduri S, Papaloizos M, Gander B (2010) Trophically and topographically functionalized silk fibroin nerve conduits for guided peripheral nerve regeneration. Biomaterials 31 (8):2323–2334
120. Xie JW et al (2009) The differentiation of embryonic stem cells seeded on electrospun nanofibers into neural lineages. Biomaterials 30(3):354–362
121. Lam HJ et al (2010) In vitro regulation of neural differentiation and axon growth by growth factors and bioactive nanofibers. Tissue Eng A 16(8):2641–2648
122. Meng J et al (2009) Enhancement of nanofibrous scaffold of multiwalled carbon nanotubes/polyurethane composite to the fibroblasts growth and biosynthesis. J Biomed Mater Res A 88 (1):105–116
123. Shang SH et al (2010) The effect of electrospun fibre alignment on the behaviour of rat periodontal ligament cells. Eur Cells Mater 19:180–192
124. Chua KN et al (2006) Surface-aminated electrospun nanofibers enhance adhesion and expansion of human umbilical cord blood hematopoietic stem/progenitor cells. Biomaterials 27(36):6043–6051
125. Sangsanoh P et al (2007) In vitro biocompatibility of schwann cells on surfaces of biocompatible polymeric electrospun fibrous and solution-cast film scaffolds. Biomacromolecules 8 (5):1587–1594
126. Chen M et al (2007) Role of fiber diameter in adhesion and proliferation of NIH 3T3 fibroblast on electrospun polycaprolactone scaffolds. Tissue Eng 13(3):579–587
127. Rubenstein D et al (2007) Bioassay chamber for angiogenesis with perfused explanted arteries and electrospun scaffolding. Microcirculation 14(7):723–737
128. McKenzie JL et al (2004) Decreased functions of astrocytes on carbon nanofiber materials. Biomaterials 25(7–8):1309–1317
129. Elias KL, Price RL, Webster TJ (2002) Enhanced functions of osteoblasts on nanometer diameter carbon fibers. Biomaterials 23(15):3279–3287
130. Baker BM, Mauck RL (2007) The effect of nanofiber alignment on the maturation of engineered meniscus constructs. Biomaterials 28(11):1967–1977
131. Lu H et al (2009) Growth of outgrowth endothelial cells on aligned PLLA nanofibrous scaffolds. J Mater Sci Mater Med 20(9):1937–1944
132. Meng J et al (2010) Electrospun aligned nanofibrous composite of MWCNT/polyurethane to enhance vascular endothelium cells proliferation and function. J Biomed Mater Res A 95 (1):312–320
133. Lee CH et al (2005) Nanofiber alignment and direction of mechanical strain affect the ECM production of human ACL fibroblast. Biomaterials 26(11):1261–1270
134. Liu Y et al (2009) Effects of fiber orientation and diameter on the behavior of human dermal fibroblasts on electrospun PMMA scaffolds. J Biomed Mater Res A 90A(4):1092–1106
135. Li WJ, Jiang YJ, Tuan RS (2006) Chondrocyte phenotype in engineered fibrous matrix is regulated by fiber size. Tissue Eng 12(7):1775–1785
136. Liu Y et al (2009) Control of cell migration in two and three dimensions using substrate morphology. Exp Cell Res 315(15):2544–2557
137. Chua KN et al (2005) Stable immobilization of rat hepatocyte spheroids on galactosylated nanofiber scaffold. Biomaterials 26(15):2537–2547
138. Shih YR et al (2006) Growth of mesenchymal stem cells on electrospun type I collagen nanofibers. Stem Cells 24(11):2391–2397
139. Johnson J et al (2009) Quantitative analysis of complex glioma cell migration on electrospun polycaprolactone using time-lapse microscopy. Tissue Eng Part C Methods 15(4):531–540
140. Pham QP, Sharma U, Mikos AG (2006) Electrospun poly(epsilon-caprolactone) microfiber and multilayer nanofiber/microfiber scaffolds: characterization of scaffolds and measurement of cellular infiltration. Biomacromolecules 7(10):2796–2805

141. Balguid A et al (2009) Tailoring fiber diameter in electrospun poly(epsilon-caprolactone) scaffolds for optimal cellular infiltration in cardiovascular tissue engineering. Tissue Eng A 15(2):437–444
142. Kurpinski KT et al (2010) The effect of fiber alignment and heparin coating on cell infiltration into nanofibrous PLLA scaffolds. Biomaterials 31(13):3536–3542
143. Cao HQ et al (2010) The topographical effect of electrospun nanofibrous scaffolds on the in vivo and in vitro foreign body reaction. J Biomed Mater Res A 93A(3):1151–1159
144. Nur EKA et al (2006) Three-dimensional nanofibrillar surfaces promote self-renewal in mouse embryonic stem cells. Stem Cells 24(2):426–433
145. Yin Z et al (2010) The regulation of tendon stem cell differentiation by the alignment of nanofibers. Biomaterials 31(8):2163–2175
146. Huber A, Pickett A, Shakesheff KM (2007) Reconstruction of spatially orientated myotubes in vitro using electrospun, parallel microfibre arrays. Eur Cells Mater 14:56–63
147. Dang JM, Leong KW (2007) Myogenic induction of aligned mesenchymal stem cell sheets by culture on thermally responsive electrospun nanofibers. Adv Mater Deerfield 19(19):2775–2779
148. Lee MR et al (2010) Direct differentiation of human embryonic stem cells into selective neurons on nanoscale ridge/groove pattern arrays. Biomaterials 31(15):4360–4366
149. Leong MF et al (2009) Effect of electrospun poly(D, L-lactide) fibrous scaffold with nanoporous surface on attachment of porcine esophageal epithelial cells and protein adsorption. J Biomed Mater Res A 89(4):1040–1048
150. Baker SC, Southgate J (2008) Towards control of smooth muscle cell differentiation in synthetic 3D scaffolds. Biomaterials 29(23):3357–3366
151. Silva GA et al (2004) Selective differentiation of neural progenitor cells by high-epitope density nanofibers. Science 303(5662):1352–1355
152. McBeath R et al (2004) Cell shape, cytoskeletal tension, and RhoA regulate stem cell lineage commitment. Dev Cell 6(4):483–495
153. Spiegelman BM, Ginty CA (1983) Fibronectin modulation of cell shape and lipogenic gene expression in 3T3-adipocytes. Cell 35(3 Pt 2):657–666
154. Maniotis AJ, Chen CS, Ingber DE (1997) Demonstration of mechanical connections between integrins, cytoskeletal filaments, and nucleoplasm that stabilize nuclear structure. Proc Natl Acad Sci USA 94(3):849–854
155. Thomas CH et al (2002) Engineering gene expression and protein synthesis by modulation of nuclear shape. Proc Natl Acad Sci USA 99(4):1972–1977
156. McBride SH, Knothe ML (2008) Tate. Modulation of stem cell shape and fate A: the role of density and seeding protocol on nucleus shape and gene expression. Tissue Eng A 14(9):1561–1572
157. Hu W, Huang ZM (2010) Biocompatibility of braided poly(L-lactic acid) nanofiber wires applied as tissue sutures. Polym Int 59(1):92–99
158. Valmikinathan CM et al (2008) Novel nanofibrous spiral scaffolds for neural tissue engineering. J Neural Eng 5(4):422–432
159. Chew SY et al (2007) Aligned protein-polymer composite fibers enhance nerve regeneration: a potential tissue-engineering platform. Adv Funct Mater 17(8):1288–1296
160. Horne MK et al (2010) Three-dimensional nanofibrous scaffolds incorporating immobilized BDNF promote proliferation and differentiation of cortical neural stem cells. Stem Cells Dev 19(6):843–852
161. Hou XX et al (2008) Stretching-induced orientation to improve mechanical properties of electrospun pan nanocomposites. Int J Mod Phys B 22(31–32):5913–5918
162. Yoon H et al (2010) Fabricating highly aligned electrospun poly(epsilon-caprolactone) micro/nanofibers for nerve tissue regeneration. Polymer-Korea 34(3):185–190
163. Koh HS et al (2010) In vivo study of novel nanofibrous intra-luminal guidance channels to promote nerve regeneration. J Neural Eng 7(4):046003
164. Zhu YB et al (2010) Macro-alignment of electrospun fibers for vascular tissue engineering. J Biomed Mater Res B Appl Biomater 92B(2):508–516

165. Zhang XH et al (2009) Dynamic culture conditions to generate silk-based tissue-engineered vascular grafts. Biomaterials 30(19):3213–3223
166. Xu CY et al (2004) Aligned biodegradable nanotibrous structure: a potential scaffold for blood vessel engineering. Biomaterials 25(5):877–886
167. Uttayarat P et al (2010) Micropatterning of three-dimensional electrospun polyurethane vascular grafts. Acta Biomater 6(11):4229–4237
168. Hashi CK et al (2007) Antithrombogenic property of bone marrow mesenchymal stem cells in nanofibrous vascular grafts. Proc Natl Acad Sci USA 104(29):11915–11920
169. He W et al (2006) Biodegradable polymer nanofiber mesh to maintain functions of endothelial cells. Tissue Eng 12(9):2457–2466
170. Han ZZ et al (2008) Growing behavior of endothelial cells on electrospun aligned nanofibrous film of polyurethane. Chem J Chin Univer-Chin 29(5):1070–1073
171. Jose MV et al (2010) Aligned bioactive multi-component nanofibrous nanocomposite scaffolds for bone tissue engineering. Macromol Biosci 10(4):433–444
172. Chen F et al (2010) Hydroxyapatite nanorods/poly(vinyl pyrolidone) composite nanofibers, arrays and three-dimensional fabrics: electrospun preparation and transformation to hydroxyapatite nanostructures. Acta Biomater 6(8):3013–3020
173. Jose MV et al (2009) Fabrication and characterization of aligned nanofibrous PLGA/Collagen blends as bone tissue scaffolds. Polymer 50(15):3778–3785
174. Jose MV et al (2009) Aligned PLGA/HA nanofibrous nanocomposite scaffolds for bone tissue engineering. Acta Biomater 5(1):305–315
175. Xie JW et al (2010) "Aligned-to-random" nanofiber scaffolds for mimicking the structure of the tendon-to-bone insertion site. Nanoscale 2(6):923–926
176. Subramanian A et al (2004) Synthesis and evaluation of scaffolds prepared from chitosan fibers for potential use in cartilage tissue engineering. Biomed Sci Instrum 40:117–122
177. Subramanian A et al (2005) Preparation and evaluation of the electrospun chitosan/PEO fibers for potential applications in cartilage tissue engineering. J Biomater Sci Polym Ed 16(7):861–873
178. Baker BM et al (2009) Tissue engineering with meniscus cells derived from surgical debris. Osteoarthritis Cartilage 17(3):336–345
179. Nerurkar NL, Elliott DM, Mauck RL (2007) Mechanics of oriented electrospun nanofibrous scaffolds for annulus fibrosus tissue engineering. J Orthop Res 25(8):1018–1028
180. Yeganegi M, Kandel RA, Santerre JP (2010) Characterization of a biodegradable electrospun polyurethane nanofiber scaffold: mechanical properties and cytotoxicity. Acta Biomater 6(10):3847–3855
181. Sell SA, McClure MJ, Ayres CE, Simpson DG, Bowlin GL (2011) Preliminary investigation of airgap electrospun silk-fibroin-based structures for ligament analogue engineering. J Biomater Sci Polym Ed 22:1253–1273
182. Wu H et al (2010) Electrospinning of small diameter 3-D nanofibrous tubular scaffolds with controllable nanofiber orientations for vascular grafts. J Mater Sci Mater Med 21(12): 3207–3215
183. Silber JS et al (2003) Donor site morbidity after anterior iliac crest bone harvest for single-level anterior cervical discectomy and fusion. Spine (Phila Pa 1976) 28(2):134–139
184. Mankin HJ, Hornicek FJ, Raskin KA (2005) Infection in massive bone allografts. Clin Orthop Relat Res 432:210–216
185. Li X et al (2008) Coating electrospun poly(epsilon-caprolactone) fibers with gelatin and calcium phosphate and their use as biomimetic scaffolds for bone tissue engineering. Langmuir 24(24):14145–14150
186. Ngiam M et al (2009) The fabrication of nano-hydroxyapatite on PLGA and PLGA/collagen nanofibrous composite scaffolds and their effects in osteoblastic behavior for bone tissue engineering. Bone 45(1):4–16
187. Teo W-E et al (2007) A dynamic liquid support system for continuous electrospun yarn fabrication. Polymer 48(12):3400–3405

188. Hu W, Huang ZM, Liu XY (2010) Development of braided drug-loaded nanofiber sutures. Nanotechnology 21(31):315104
189. Meek KM, Boote C (2004) The organization of collagen in the corneal stroma. Exp Eye Res 78(3):503–512
190. Baker BM et al (2008) The potential to improve cell infiltration in composite fiber-aligned electrospun scaffolds by the selective removal of sacrificial fibers. Biomaterials 29(15):2348–2358
191. Beachley V, Wen XJ (2009) Fabrication of nanofiber reinforced protein structures for tissue engineering. Mater Sci Eng C 29(8):2448–2453
192. Wang W et al (2009) Effects of Schwann cell alignment along the oriented electrospun chitosan nanofibers on nerve regeneration. J Biomed Mater Res A 91A(4):994–1005